Autecology and Genetic Diversity of *Cletocamptus* Copepods in Coastal Hypersaline Lagoons of Puerto Rico

Jean P. Domenech Ramos[1],*, Paulo Corgosinho[2], and Nikolaos V. Schizas[1]

[1]*University of Puerto Rico at Mayagüez, Department of Marine Sciences, Mayagüez, Puerto Rico, U. S. A.*
[2]*Laboratório de Microscopia e Ecologia de Vetores de Doenças, Universidade Estadual de Montes Claros, Montes Claros, Minas Gerais, Brasil*

*Corresponding author: jean.domenech2@upr.edu

Abstract—Copepods of the genus *Cletocamptus* are common inhabitants of coastal saline lagoons of the greater Caribbean. They are abundant in southern Puerto Rico, where past studies indicate the presence of one species, *Cletocamptus dominicanus*; but genetic and ecological studies have yet to be conducted. For a year, we surveyed the *Cletocamptus* populations of three lagoons (Candelaria, Fraternidad, and Playa Sucia) in southwestern Puerto Rico. Densities fluctuated within and between lagoons, suggesting patchy distribution. Their density ranged from 0 to 486 copepods/cm² of sediment. Salinity, temperature, and pH were not correlated with copepod densities, suggesting tolerance to environmental fluctuations. Specimens exhibited morphological variability, motivating us to assess the standing genetic variability and the potential of cryptic species by employing two molecular markers. The mitochondrial COI and the nuclear ribosomal 28S genes were sequenced from 130 and 118 specimens, respectively, collected from Candelaria, Fraternidad, and Playa Sucia, as well as from an additional four lagoons (Petrona, Encarnación, Providencia, and Flamenco). Phylogenetic analyses using both genes indicate the presence of at least four lineages. Based on COI sequences, corrected sequence divergence between the lineages ranged from 13% to 43%. Given the large sequence divergence among the *Cletocamptus* lineages, we used single-locus species delimitation tools (GMYC, bPTP, mPTP, ASAP, and ABGD) to assess for the presence of additional species beyond the previously reported *C. dominicanus*. Most delimitation tests grouped taxa into five putative species. *Cletocamptus* spp. are often the numerically dominant benthic metazoans in these important coastal habitats and warrant taxonomic, genomic, and physiological studies to understand their divergence and adaptations to this unique environment.

Copepods are the most abundant metazoans in the marine environment and are highly diverse, with ~14,000 described species (Turner 2004; WoRMS Editorial Board 2024). They fulfill essential roles in marine and freshwater ecosystems by promoting bioturbation by reworking sediments, driving food web dynamics by linking primary producers to larger metazoans, and having important roles in the global carbon and nitrogen cycles (Hicks and Coull 1983; Frangoulis et al. 2004; Schratzberger and Ingels 2018). They are ubiquitous throughout the planet, and are found in nearly all habitats with water, including extreme environments like the deep sea, glaciers, and hypersaline waters (Kikuchi 1994; Anufriieva 2015; Rosli et al. 2018).

Harpacticoida alone has ~3,600 described species (Suárez-Morales 2015), and estimates for total diversity could reach 150,000 species (Seifried 2004). Within

the Harpacticoida, members of the genus *Cletocamptus* (Fig. 1) are of interest for their remarkable ability to inhabit a range of salinities, from freshwater (Gómez et al. 2007) to extreme environments like hypersaline lagoons (Súarez-Morales et al. 2013; Anufriieva 2015; Gómez et al. 2017; Yakovenko et al. 2024). These euryhaline organisms are found in many habitats worldwide, most commonly in estuaries and saline lagoons (Gómez et al. 2004, 2013; Anufriieva 2014). This is observed in the greater Caribbean, where they are considered the most abundant harpacticoid inhabiting coastal saline lagoons (Gómez et al. 2017).

Taxonomic work and species assignment within the genus is difficult due to incomplete or erroneous species descriptions in the early years (e.g., *C. dominicanus, C. deitersi, and C. albuquerquensis* had to be redescribed by Gómez et al. (2017)). *Cletocamptus*

FIG. 1. Confocal laser microscopy of *Cletocamptus* specimens found in this study. Specimens stained using Congo red following the protocol of Michels and Büntzow (2010). Each copepod is labeled with its id; specimens 15_13 and 3_70 are from Lineage 1, 0_220 is from Lineage 1c, and 13_81 is from Lineage 3, as labelled in the COI ML phylogeny.

also has cryptic species (Rocha-Olivares et al. 2001), and some species exhibit high intraspecific morphological variability (Fleeger 1980; Castro-Longoria et al. 2003; Gómez and Yáñez-Rivera 2022). Gómez and Yáñez-Rivera (2022) have done the most comprehensive morphological phylogenetic work in revising the genus, with 27 recognized species.

Only a single species, *Cletocamptus dominicanus,* has been reported in the coastal lagoons of Puerto Rico, where they have been found in salinities of up to 87.6 psu (Gómez et al. 2017). Additionally, only two publications, viz. Castro-Longoria et al. (2003) and Rocha-Olivares et al. (2001) focus on the genetic diversity within the genus *Cletocamptus*. This study aims to enhance our understanding of the ecology and systematics of *Cletocamptus* copepods in Puerto Rico by sampling several coastal lagoons and leveraging molecular phylogenetic tools to delineate lineages of *Cletocamptus* from the island.

MATERIALS AND METHODS

Area of study

The first portion of this work investigates the population dynamics of *Cletocamptus* in three lagoons within the Cabo Rojo National Wildlife Refuge, namely Candelaria (CL), Fraternidad (FL), and Playa Sucia lagoons (SL) (Fig. 2I) (Permits DNER 2020-IC-059 and USFW 2020-04). These lagoons within the Cabo Rojo National Wildlife Reserve are an important stopover in the Caribbean for migrating shorebirds (Collazo et al. 1995), including the stilt sandpiper (*Calidris himantopus*) and the black-necked stilt (*Himantopus mexicanus*) (Parks et al. 2016). The lagoons are heavily impacted, as they are thought to have been used for salt extraction since 700 AD. Their topography has been altered to make evaporation basins, where the water level is managed for salt production rather than left to fluctuate naturally.

FIG. 2. Area of study; I. Inset map includes lagoons of the Cabo Rojo National Wildlife Refuge used for the demographic portion of the study. Lagoon sites are represented by the first letter of their names (C = Candelaria, F = Fraternidad, S = [Playa] Sucia) along with letters (A, B, and C) indicating specific sampling areas; II. The island of Puerto Rico and the lagoons included in the genetic analyses.

The second portion of this work investigates the genetic diversity of *Cletocamptus* copepods in shallow coastal lagoons with elevated salinities at the time of sampling, including the aforementioned Cabo Rojo lagoons (> 41 psu) and four additional sites, namely, Providencia (45 psu), Encarnación (75 psu), Petrona (61 psu), and Flamenco lagoons (40 psu) (Fig. 2II). All are located on the southern coast of Puerto Rico, except for Flamenco Lagoon, which is located on Culebra Island, about 25 km East of the eastern coast of Puerto Rico.

Demographics

Samples were collected from Candelaria, Fraternidad, and Playa Sucia lagoons (Fig. 2I). at a randomly selected date each month, from January 2020 to February 2021, with a gap in April–June 2020 due to the COVID-19 crisis (total of 10 sampling dates). Each lagoon was sampled in three areas (denominated A, B, and C), considering accessibility to the lagoon and intending to sample different areas (Fig. 2I).

Three sediment samples were collected with a sediment corer (5 cm² area, 10 cm³ volume) from three areas of each lagoon, i.e., nine sediment cores were collected from each lagoon at each sampling time. For easier accessibility, only the lagoon borders were sampled, where water depths ranged from 8 to 15 cm. Each core was stored in a 50 ml centrifuge tube, then sifted with a 125 μm sieve and preserved in 95% EtOH with rose bengal to facilitate visualization of meiofauna. Each

core was then divided into eight subsamples using a modified Jensen meiofauna sample splitter (Jensen 1982). Two of the subsamples from the meiofauna splitter were inspected with a Nikon SMZ800 dissection microscope. Individuals of *Cletocamptus* were counted and categorized as female, gravid female, male, or copepodid. Nauplii were seldom seen due to the sieve size (125 μm) used and are not included in this study. Three abiotic parameters (temperature, pH, and salinity) were measured in all lagoon areas at each sampling time. Temperature and salinity were measured in situ with a field thermometer and refractometer; pH was measured with a SevenEasy Metler Toledo pH meter in the laboratory using water samples from each lagoon area.

The data from the two subsamples were extrapolated to estimate the abundance of the whole sample by multiplying the counted copepod abundances by four since there were eight subsamples in the meiofauna splitter. This was used to generate an Euclidian distance resemblance matrix. The matrix was used for a PERMANOVA using PRIMER v. 7 (Anderson et al. 2008; Clarke and Gorley 2015), to test whether the factors *date*, *lagoon*, and *area* (nested in lagoon) affected the variance of *Cletocamptus*' abundance. A biotic and environmental matching analysis (BIOENV) within PRIMER was also conducted to correlate environmental variables (salinity, pH, and temperature) with the abundance of *Cletocamptus*. BIOENV is a multivariate correlation analysis weighted by season (rainy vs. dry).

After examining collected copepods under a dis-

TABLE 1. Primer pairs used in this study.

Primer Pairs (5'–3')	Gene	Product Size	Annealing Temperature	Author(s)
dgLCO1490: ggtcaacaaatcataaagayatygg dgHCO2198: taaacttcagggtgaccaaaraayca	COI	614 bp	47° C	(Meyer 2003)
LCO1490: ggtcaacaaatcataaagatattgg Cop-CO1-2189R: gggtgaccaaaaaatcaraa	COI	580 bp	45° C	(Folmer et al. 1994) (Bucklin et al. 2010)
mlCO1intF: ggwacwggwtgaacwgtwtayccycc jgHCO2198: taiacytciggrtgiccraaraayca	COI	313 bp	54° C	(Leray et al. 2013) (Geller et al. 2013)
28S-F1a: gcggaggaaaagaaactaac 28S-R1a:gcatagtttcaccatctttcggg	28S	800 bp	51° C	(Ortman 2008)

secting microscope, we noticed high morphological variability, which suggested the possibility of more than one *Cletocamptus* species. This observation motivated us to use DNA sequencing to test whether several genetic lineages/species of *Cletocamptus* are present in the coastal lagoons of Puerto Rico.

Molecular work: DNA extraction, amplification, and sequencing

Copepods were collected from the sediment of the three Cabo Rojo Lagoons, four coastal lagoons of southern Puerto Rico and one lagoon from Culebra Island (Fig. 2) (Permits DNER 2020-IC-059 and USFW 2020-04). Sediment was obtained by scraping the lagoon bottom with a bottle, the sediment was then sifted in situ with a 125 µm sieve and preserved with 95% EtOH. To extract genomic DNA, individual copepods from each location were transferred from EtOH storage to dH$_2$O for about 10 minutes at room temperature to eliminate the majority of EtOH, a possible amplification inhibitor. Each sample was labeled with its location code (0: Cabo Rojo National Wildlife Refuge (i.e., Fraternidad, Candelaria, and Playa Sucia lagoons); 3: Providencia 6: Encarnación; 13: Petrona Point; and 15: Flamenco lagoon on Culebra Island) and the extraction number. Individual copepods were placed in 0.5 ml microcentrifuge tubes with ~20 µl of 5% Chelex 100 or InstaGene Matrix (Bio-Rad Laboratories). Samples were cooled on ice for about 10 minutes, vortexed for 15 seconds, quickly centrifuged to accumulate material at the bottom of the tube, heated to 99° C for 10 minutes, vortexed for 15 seconds, and finally centrifuged at 12,000 rcf for 3 minutes. Afterwards, the Chelex resin and the exoskeleton of the copepod precipitates on the bottom of the tube, and the DNA containing supernatant is used for PCR. The exoskeleton was retrieved and preserved in formalin for morphological observations.

Genetic variability among the processed specimens was tested using two genes with differing evolutionary drivers (Hellberg 2009). The molecular markers used are a mitochondrial and a nuclear ribosomal gene, i.e., cytochrome *c* oxidase subunit I (COI) and large nuclear subunit (28S) rRNA. COI is the de facto marker in biodiversity studies of metazoans and has been successfully used in population genetics and low-level phylogenetic studies (Rocha-Olivares et al. 2001; Machida et al. 2006; Adamowicz et al. 2010; Garlitska et al. 2012). The 28S gene is more appropriate for higher-level phylogenetic studies (more conserved), but could still provide important insights when closely related cryptic species/lineages are expected to be discovered when used with other molecular markers. Various COI primers (see Table 1) were used due to the difficulty amplifying some specimens. PCR was performed using Bio-Rad T100 Thermal Cyclers. A reaction volume of 20 µl consisted of 10 µl of Kapa Taq ReadyMix 2x (Roche), 0.15–0.45 µl of 10 mMol primer (reverse and forward), 1–3 µl of template DNA, and PCR grade H$_2$O to complete the desired volume. If reaction volumes changed, components changed proportionally. Annealing temperature gradients were performed to verify optimal annealing temperatures. PCR cycles included: initial denaturation at 95° C for 3 minutes; 35 cycles of denaturation at 95° C for 30 seconds, (see Table 1), and extension at 72° C for 1 minute/kb; the last step is a final extension at 72° C for 1 minute/kb. The success of PCR amplifications was verified using gel electrophoresis on a 1% agarose gel run at ~74 V for 30 minutes. Amplicons were sent to McLab Sequencing Facility (San Francisco, CA) for Sanger sequencing.

Sequence processing

The resulting DNA traces were inspected and edited using CodonCode Aligner v. 10.00.02 or AliView (Larsson 2014). Individual sequences were blasted using the blastn tool on NCBI (Altschul et al. 1990) to test for homology and possible contamination. All contaminated or low-quality sequences were discarded (about 70%). A sequence alignment for each gene was then created using the online version of MAFFT v. 7 (Katoh et al. 2019) and trimmed with trimAl (Capella-Gutiérrez et al. 2009). Available *Cletocamptus* COI sequences (AF315014, AF315012, AF315009, AF315011, AF315010; Rocha-Olivares et al. 2001) were also included in the analyses. *Enhydrosoma curticauda* (MH976577), *Stenocaris* sp. (MF077882), and *Laophontodes* sp. (MF077876) were used as outgroups for phylogenetic analysis of COI. *Cletodidae* sp. (MF077804), *Stenocaris* sp. (MF077862), and *Paralaophonte meinerti* (KR048898) were used as outgroups for the phylogenetic analysis of 28S. Except for *Stenocaris* sp., no other harpacticoid species existed with NCBI records for both genes; instead, we used outgroup taxa that at least belonged to the same families. All sequences produced from this study were submitted to GenBank (Appendix 1).

Phylogenetic inference

ModelFinder (Kalyaanamoorthy et al. 2017) was used, within IQ-TREE (Minh et al. 2020) to estimate the best-fit nucleotide substitution model for each dataset according to the Bayesian Information Criterion (BIC). Single gene phylogenies were estimated using maximum likelihood (ML) analysis with 100 non-parametric bootstraps. Multigene phylogenetic analysis was made by concatenating COI and 28S sequences with SequenceMatrix v. 1.9, partitioning the data by gene and constructing the phylogeny with IQ-TREE. The resulting trees were visualized using iTOL (Letunic and Bork 2021). The major clades from the COI ML phylogeny were identified, and then the 'between group mean distances' of these clades were calculated using MEGA11 (Tamura et al. 2021). Analyses were performed with 1,000 bootstrap replications, using p-distances and Tamura 3-parameter nucleotide substitution model, allowing for transitions and transversions, alpha parameter of Gamma distribution equal to 1, heterogenous patterns among lineages, and pairwise deletion of gaps/missing data.

Species delimitation

Various molecular tests were performed to delimit possible species using the COI dataset, i.e., ASAP (Puillandre et al. 2021), ABGD (Puillandre et al. 2012), mPTP (Kapli et al. 2017), bPTP (Zhang et al. 2013), and GYMC. Online versions of ABGD (https://bioinfo.mnhn.fr/abi/public/abgd/abgdweb.html) and ASAP (Puillandre et al. 2021; https://bioinfo.mnhn.fr/abi/public/asap/asapweb.html) were used with the JC69 model and default parameters. Online versions of mPTP (https://mptp.h-its.org/#/tree; Kapli et al. 2017) and bPTP (https://species.h-its.org/; Zhang et al. 2013) were used. The bionj tree from IQ-TREE was used as input for mPTP. A BI consensus tree constructed with MrBayes was used for the bPTP method. MrBayes v. 3.2.7 (Huelsenbeck and Ronquist 2001) was used for BI, analysis was run for 3×10^6 generations, sampling every 1,000 chains, with a 25% burn-in. To run a GMYC (Generalized mixed Yule-coalescent) test (Fujisawa and Barraclough 2013), ultrametric trees were generated using BEAST2 with different parameters, i.e., yule model with constant clock, yule with relaxed clock, and coalescent model with constant population and constant clock, all with a rate of evolution set to 1 (Michonneau 2016), with 10,000,000 reps and with the BModelAnalyzer package. Consensus trees were generated using TreeAnnotator with 10% burning. GMYC was implemented using the *splits* v. 1.0.20 (Ezard et al. 2021) package for R v. 4.2.2 (RStudio Team 2020; R Core Team 2021).

RESULTS AND DISCUSSION

Demographics

Cletocamptus copepods were found in three lagoons of the Cabo Rojo National Wildlife Refuge (Candelaria, Fraternidad, and Playa Sucia lagoon; Fig. 2I), and their abundances and demographic composition were measured. Large fluctuations of copepod densities were observed at all lagoons throughout the one-year study (Fig. 3). High standard deviations for the total average density of copepods at each lagoon, 221 (CL), 239 (FL), and 51(SL), demonstrate high variability. This variability is also seen at the lagoon area level, exemplified by the standard error bars in Fig. 3.

Candelaria Lagoon (CL)

The highest density of copepods at any lagoon was observed for CL, 486 copepods/cm², in March, 2020
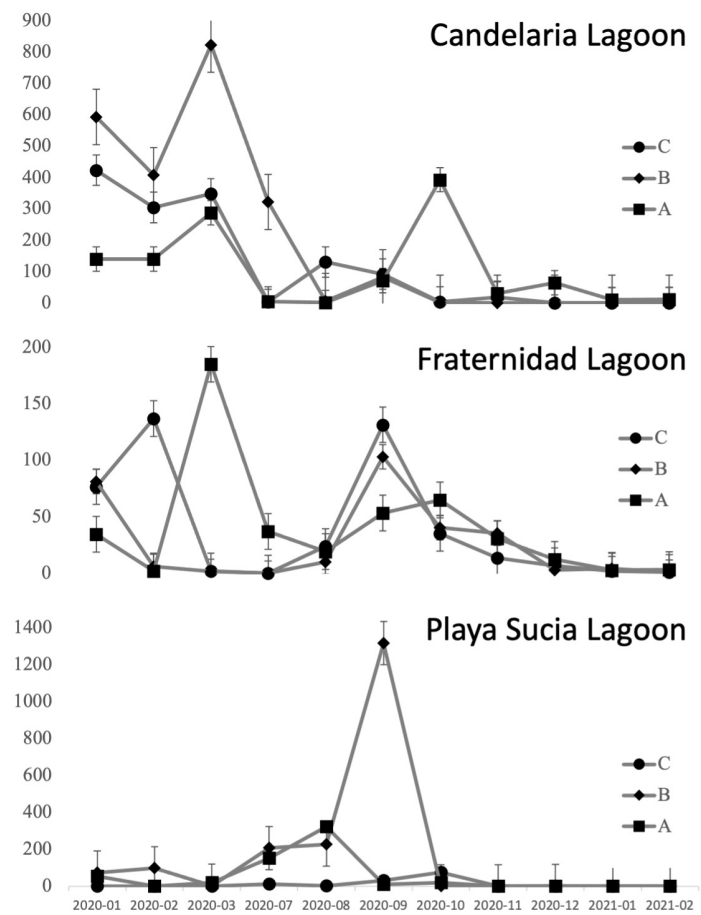
FIG. 3. The average number of *Cletocamptus* spp. per cm² in each lagoon area through time.

(Fig. 4). CL had the highest overall density (total average) of copepods with 142 copepods/cm² during the year. CL was the most productive (in terms of *Cletocamptus* copepods per area) out of the three lagoons. CL had an average of 14 gravid females per cm² in January 2020 (Fig. 4). CL also had the highest percentage of non-gravid females out of all lagoons (79.8%), but the lowest percentage of gravid females (2.7%), copepodids (8.1%), and males (9.4%) (Table 2).

Fraternidad Lagoon (FL)

The highest average density at FL was found in September, 2020, with 96 individuals/cm² (Fig. 4). FL had an overall density (total average) of 35 copepods/cm² during the year, making it the least populated of the three lagoons. FL had an average of 21 gravid females per cm² in September 2020. Fraternidad Lagoon had the lowest percentage of non-gravid females at 54.1%, however, it had the highest percentages of gravid females (13.0%), copepodids (18.3%), and males (14.6%) (Table 2).

Playa Sucia Lagoon (SL)

The highest average densities for Playa Sucia Lagoon were observed in September, 2020, the same sampling date as FL, with 452 individuals/cm² (Fig. 4). SL had an overall density (total average) of 80 copepods/cm², making it the second most populated of the three. SL had an average of 15 gravid females per cm² in July, 2020. If abundance sums for SL are turned into percentages, we can see that all demographic categories fall between the other lagoons. Non-gravid females at 67.7%, gravid females account for only 3.5%, copepodids 16.1%, while males formed 12.8% of all *Cletocamptus* counted for this lagoon (Table 2).

All lagoons have different and fluctuating densities of copepods; non-gravid females are the major demographic category, followed by copepodids, males, and gravid females (Fig. 4). Copepods are patchily distributed, as exemplified by the heterogenous column heights, and there is a stark decrease in abundance at all lagoons beginning in October, 2020 that persists to the end of sampling in February, 2021 (Fig. 4). During this period, we observed the lowest densities (e.g., 4 (CL), 2 (FL), and 0 (SL) copepods/cm²).

Using abundance data, the percentage of non-gravid females is 72.5%. Gravid females account for only 4.4%, copepodids reach a total of 12.0% of all copepods counted, while males only 11.1% (Table 2). Females were the largest demographic representative for all lagoons through time, with few exceptions (Figs. 4, 5). This is nearly a third of all copepods counted throughout this investigation. This pattern is common, as benthic harpacticoids with r-population strategies and large populations have been seen to have larger female-to-male ratios (Dahms and Qian 2004).

Even though abundances approached zero near the end of sampling, total average copepod densities were higher than what is commonly seen in other harpacticoid studies in surface sediment of shallow aquatic ecosystems, where average densities are lower than 30 copepods/cm² (Jayabarathi et al. 2015)with harpacticoids dominating (51%.

Statistical inference

In brackish systems, the abundance of harpacticoid copepods is positively correlated with increasing salinity. Copepods are less abundant in oligohaline regions, indicating a preference for higher salinity levels (Yamamuro 2000). In tropical estuaries and coastal
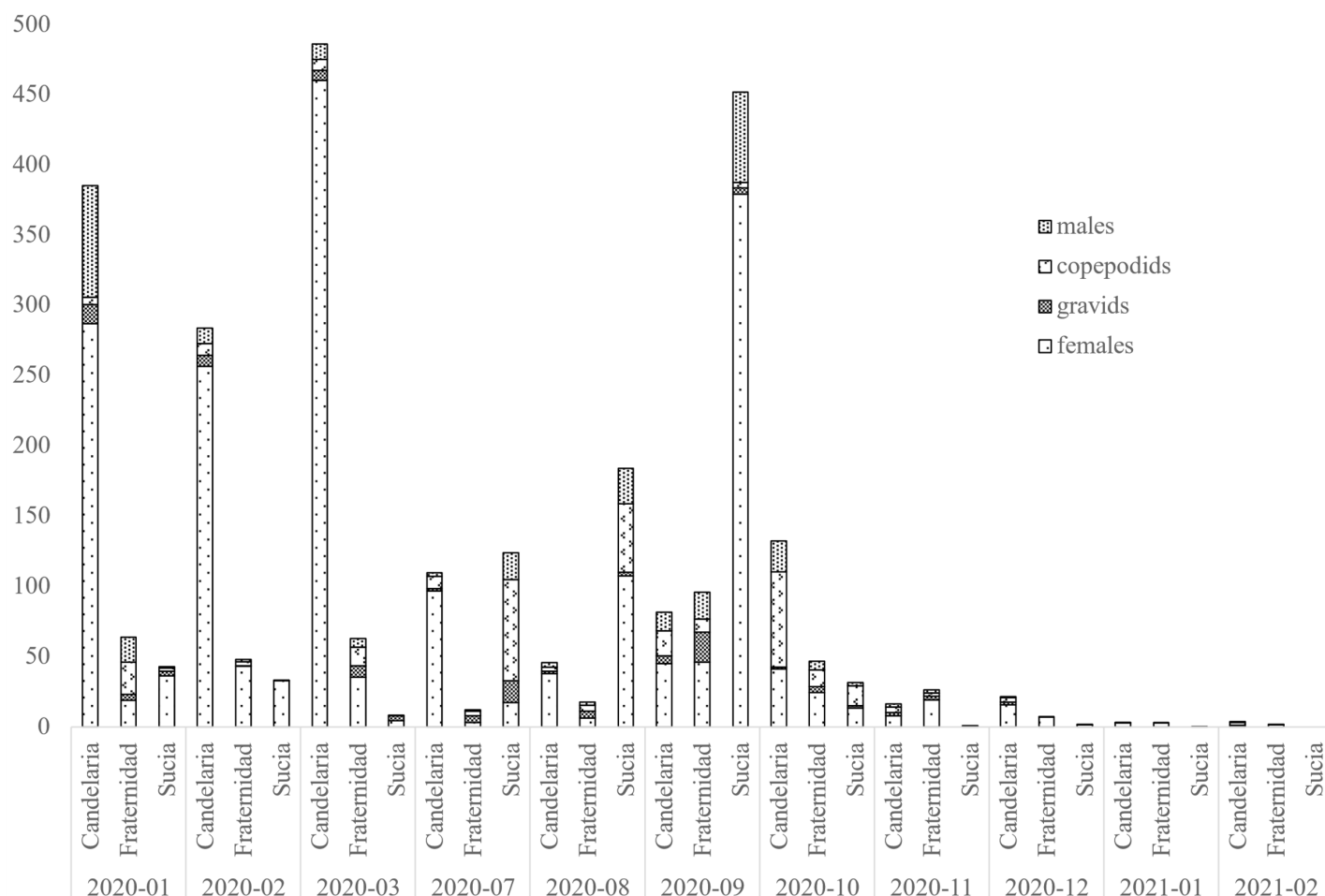
Fig. 4. Density (copepods/cm²) of *Cletocamptus* spp. at each lagoon at all sampling times.

lagoons, copepod densities are generally lower due to significant salinity fluctuations and temperature stress (Armenteros et al. 2007). Temperature plays a crucial role in the ecology of copepods as high temperatures can increase oxidative and physiological stress, affecting their reproduction and survival (Von Weissenberg et al. 2022). pH also influences copepod populations, as low levels can significantly reduce the egg production rates of certain copepod species. For example, at a pH of 7.6 compared to 7.9, the egg production rate of some copepod species decreased by approximately two-fold when combined with increased temperatures (Lee et al. 2020). Furthermore, it is hypothesized that copepods may survive in hypersaline environments by acquiring exoosmolytes through their diet, i.e., by eating osmolyte-containing algae (Shadrin and Anufriieva 2013; Anufriieva 2015). Copepod densities in shallow coastal lagoons are affected by interactions of temperature, salinity, and pH, and the ability of copepods to survive in hypersaline environments may be habitat/community dependent.

At the Cabo Rojo lagoons, we measured temperatures ranging from 22 to 42° C, salinities from 27 to150 psu, and pH from 7.25 to 9.03 (Figs. 6–8; Table 3; and for averages of all lagoons at all sampling times Appendix 2). These parameters reach extreme values, creating a challenging environment for its inhabitants, and should significantly influence the abundance of *Cletocamptus* in these lagoons. However, a BIOENV analysis shows that the interaction of salinity, temperature, and pH did not correlate with the abundance of copepods (Rho = 0.043, P = 0.87). The same analysis using only single physicochemical variables resulted in even lower correlations. That is to say, the abundance of *Cletocamptus* copepods was not correlated to any of the parameters measured, e.g., events of high salinity or temperature. A PERMANOVA test indicated there is a low probability that the observed variability of copepod densities is explained by the factors (date, lagoon, area) included in this sampling design. What best explained the variability in the abundance of *Cletocamptus* is the date x area (nested in lagoon) interaction (p = 0.001 and

TABLE 2. Demographic composition of each lagoon throughout all sampling dates.

Lagoon	Percentage (%) of			
	Females	Gravid Females	Copepodids	Males
Candelaria	79.8	2.7	8.1	9.4
Fraternidad	54.1	13.0	18.3	14.6
Playa Sucia	67.7	3.5	16.1	12.8
Total	72.5	4.4	12.0	11.1

TABLE 3. The highest and lowest parameters for each lagoon where *Cletocamptus* was present. The sampling date is included in parentheses.

Lagoon	pH		Temperature (° C)		Salinity (psu)	
	lowest	highest	lowest	highest	lowest	highest
Candelaria	8.02 (10/2020)	9.03 (01/2020)	27 (11/2020)	42 (07/2020)	27 (11/2020)	124 (02/2020)
Fraternidad	7.25 (02/2020)	8.89 (12/2020)	22 (02/2020)	38 (07/2020)	36 (01/2021)	115 (03/2020)
Playa Sucia	7.89 (08/2020)	8.97 (01/2020)	25 (11/2020)	41 (10/2020)	43 (11/2020)	95 (07/2020)

Pseudo-F = 13.211), meaning that the variability in the abundance of copepods in each area of each lagoon was independent of sampling time.

A wider sampling grid, i.e., a higher sampling effort, may have detected temporal trends by lessening the effects of patchy distributions. Notwithstanding, the absence of significant statistical results pertaining to the interaction of factors and correlations of physicochemical factors with copepod densities in this study can be attributed to temporal cycles in population size (unrelated to seasonal fluctuations), microtopography of the lagoons, sediment particle size (De Troch et al. 2006), and the patchy spatial distribution of benthic copepods. Food availability and dissolved oxygen could also affect the abundance of the small crustaceans (Alcocer et al. 2015). It can also be caused by dormancy (Dahms and Qian 2004), where resting eggs lie dormant during unfavorable periods. Additionally, abundance trends may have been obfuscated by the presence of more than one *Cletocamptus* species in our samples, as we found from our genetic surveys, which inhabit the same ecosystem but may occupy different niches with different population trends.

Phylogenetic inference

One hundred thirty (130) sequences of COI and 118 sequences of 28S were generated (GenBank Accession Numbers: COI: OQ682279–OQ682408; 28S: OQ819183–OQ819299). After editing and trimming, the final lengths of the COI and 28S sequences were 623 and 865 bp, respectively. ModelFinder suggested K3Pu+F+I+G4 (BIC score 11715.8) for COI and TN+F+G4 for 28S (BIC score 7499.7) as the best-fit substitution models according to the Bayesian Information Criterion. ML gene phylogenies were constructed to test for the presence of one or more lineages of *Cletocamptus*, based on the observed morphological variability. *Cletocamptus* from the Candelaria, Fraternidad, and Playa Sucia lagoons (of Cabo Rojo) and four other coastal saline lagoons (Providencia, Encarnación, Petrona, and Flamenco lagoons) that covered a longitudinal gradient spanning from the southwesternmost part of the main island to the easternmost part of the island archipelago were included (Fig. 2II). Additionally, we included five COI sequences from GenBank generated by Rocha-Olivares et al. (2001). The resulting phylogeny grouped local *Cletocamptus* into five major lineages (Fig. 9). One hundred and eighteen 28S sequences generated from this study were also analyzed phylogenetically (Fig. 10). The 28S ML phylogeny is more conserved and does not recover an identical structure/grouping as COI, yielding four lineages, instead of five. This has been observed in other studies where the phylogenetic structure of the tree changes with differ-
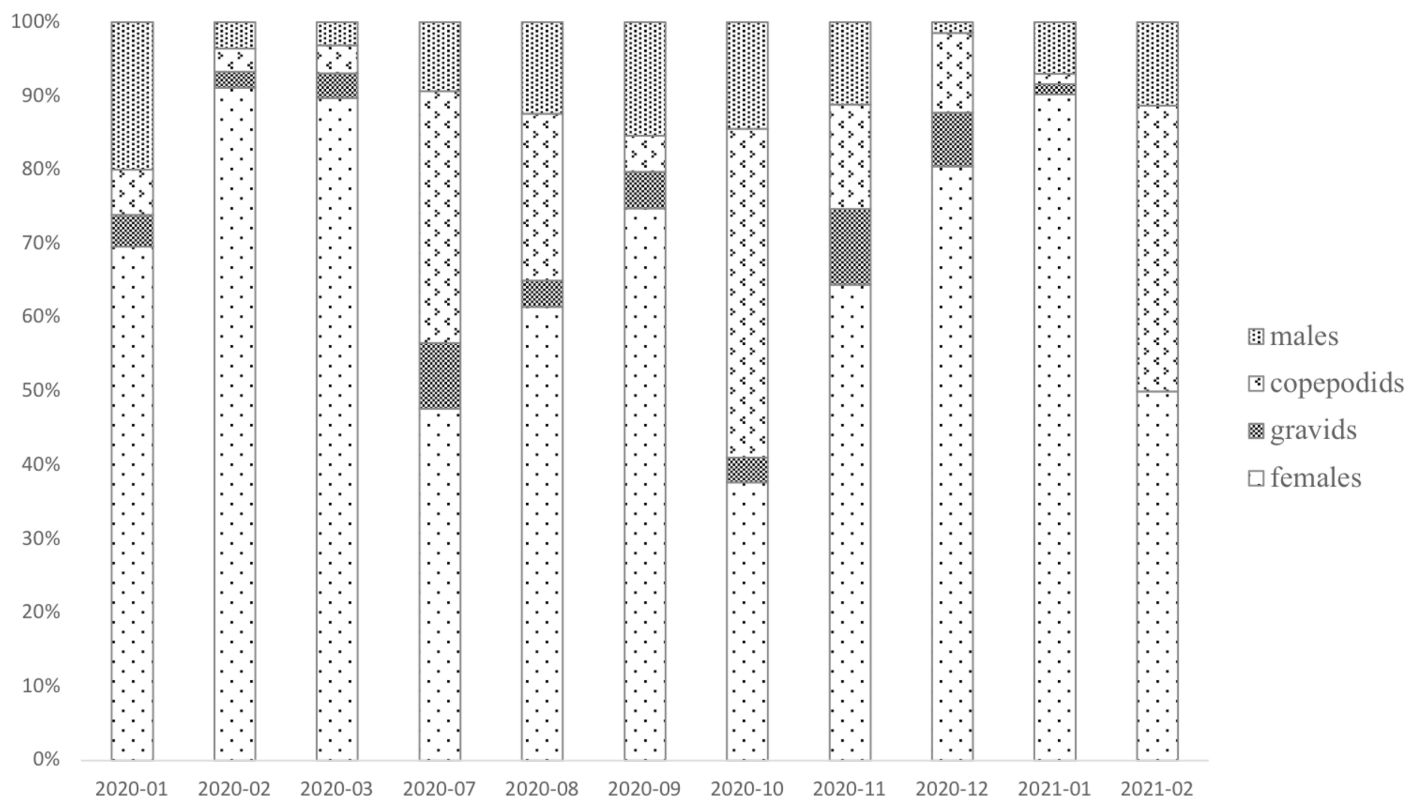
FIG. 5. Percentages of females, gravid females, copepodids, and males of *Cletocamptus* spp. sampled at all lagoons at each sampling time.

ent marker genes (González et al. 2020). The generated ML multigene (COI+28S) phylogeny recovers the same major lineages as COI (Fig. 11).

The major lineages recovered by the genetic analysis were used to create groups and estimate their genetic distances. Corrected genetic distances between these groups are high and range from 13 to 43% (Table 4). A 3% and 9% COI divergence is considered a threshold to call putative species for Coleoptera and Lepidoptera, respectively (Hebert et al. 2003; Ma et al. 2022). However, genetic distances between harpacticoid copepod species are generally higher than other arthropod taxa. The genetic distances among the *Cletocamptus* lineages concord with those between *Cletocamptus* species (Rocha-Olivares et al. 2001; Table 4) and between species of other copepod genera, such as *Enhydrosoma*, *Nannopus,* and *Tigriopus*, indicating that the major lineages recovered by the COI and multigene phylogenies could be putative species.

The multigene tree with the *Cletocamptus* specimens linked to their geographic coordinates can be seen in Fig. 11. Lineage 3 is composed solely of copepods from Punta Petrona and was recovered by both COI and 28S gene phylogenies; the recovery of all other lineag-

es varied between genes. All lineages except Lineage 3 are found in more than one sampling location. Lineage 4 is the most broadly distributed, having a presence in all sampling locations. The Cabo Rojo lagoons host Lineages 1, 2, and 4 (Table 5). All lagoons host three lineages, except for Punta Petrona, which hosts two. Most copepods from Flamenco lagoon of Culebra comprise Lineage 1, however there are also members of Lineages 4 and 5 represented. The presence of three lineages in Culebra suggests that there are no effective spatial barriers to limit genetic flow between locations of the main island of Puerto Rico and Culebra Island, which is geographically isolated by a ~35 km stretch of ocean. The mechanisms of gene flow for *Cletocamptus* across lagoons and across Caribbean islands are unknown. However, many migrating waterbirds visit these lagoons, e.g., shorebirds (Collazo et al. 1995), ducks, and egrets; it has been suggested that birds may disperse copepod eggs undigested through their feces, or whole copepods in their feet and plumage (Green and Figuerola 2005; Frisch et al. 2007; Hessen et al. 2019). Dispersal through birds is a promising hypothesis since coastal lagoons have little connection to ocean currents and *Cletocamptus* spp. as benthic harpacticoid

FIG. 6. Average temperatures for Cabo Rojo lagoons at each sampling time; C = Candelaria; F = Fraternidad; S = [Playa] Sucia Lagoon.
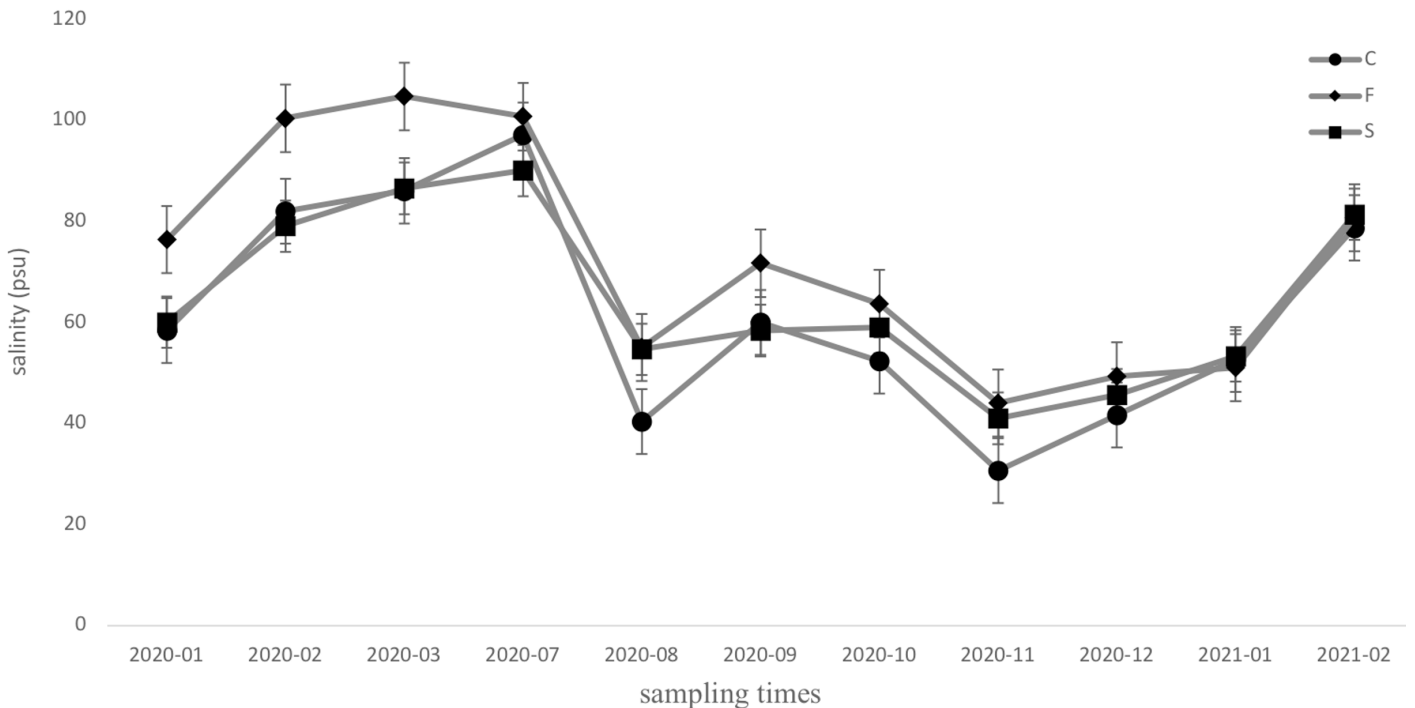
FIG. 7. Average salinity (psu) for Cabo Rojo lagoons at each sampling time; C = Candelaria; F = Fraternidad; S = [Playa] Sucia.

species have obligatory benthic nauplii, making dispersal through this route highly improbable.

From an ecological perspective, the potential for spatial barriers to drive genetic differentiation and speciation in aquatic organisms such as copepods has important implications for conservation and management. Understanding the distribution and connectivity of populations can inform conservation efforts by identifying areas of high genetic diversity and evolutionary potential. Furthermore, the ecological context in which
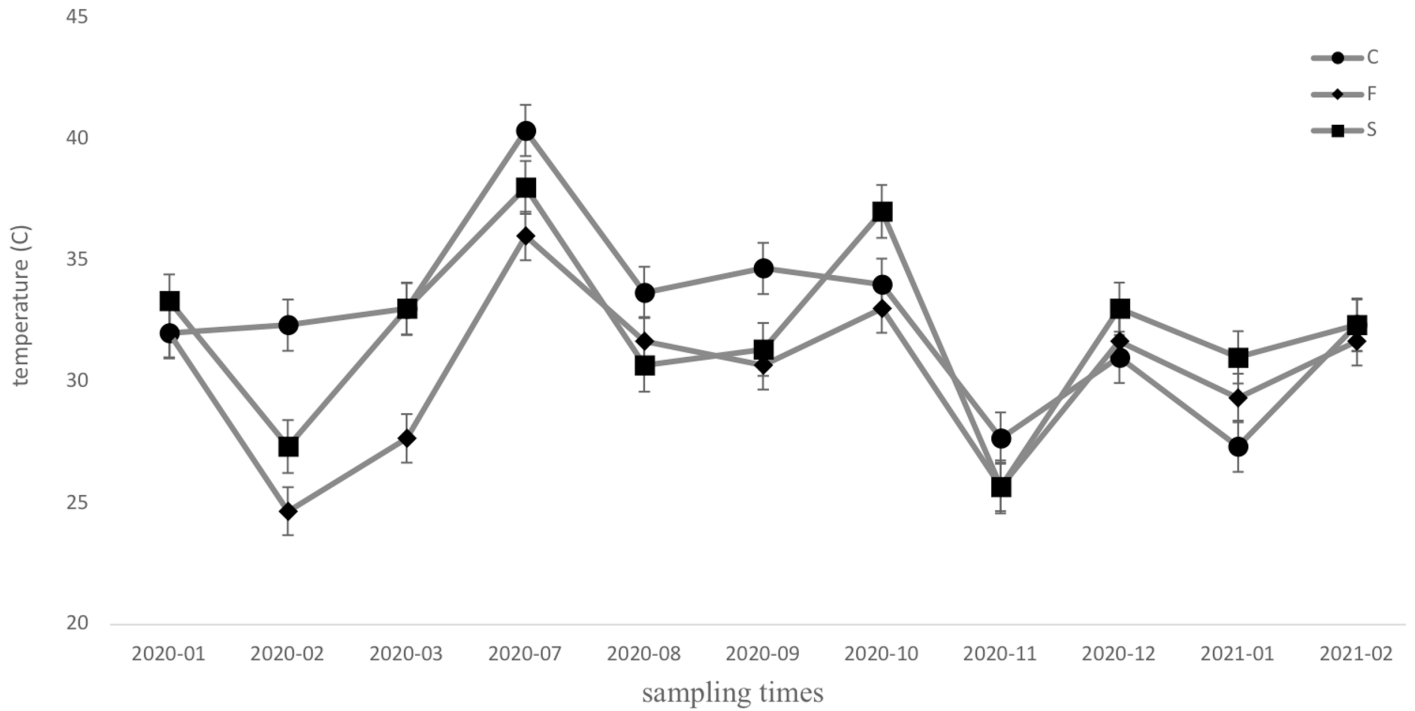
Fig. 8. Average pH for Cabo Rojo lagoons at each sampling time; C = Candelaria; F = Fraternidad; S = [Playa] Sucia.

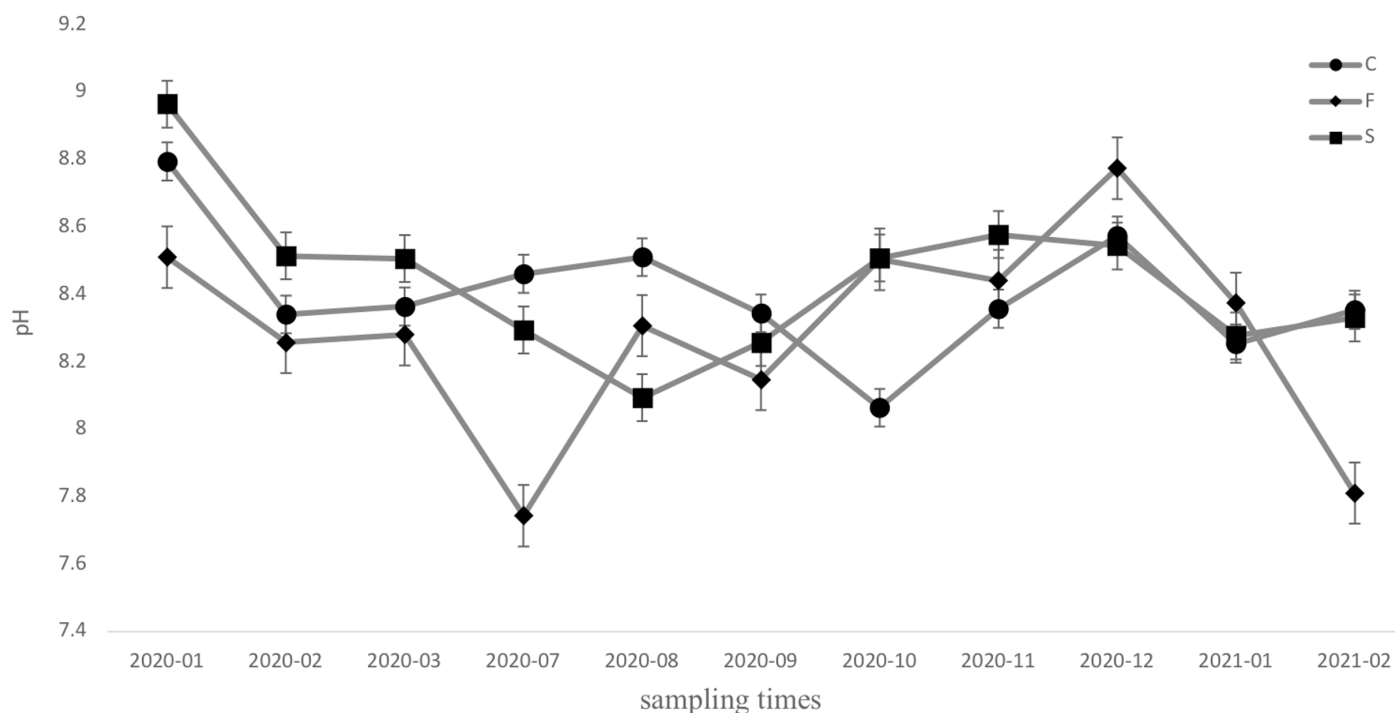organisms live can also affect their evolution and diversity. In the case of *Cletocamptus*, the saline lagoon habitat may play a critical role in driving the genetic differentiation of these copepods. Understanding which factors drive genetic differentiation can help us better understand how species evolve and adapt to changing conditions over time.

Species delimitation

Species delimitation tests were conducted using 135 COI sequences (Fig. 9). The ASAP delimitation test creates partitions that range from nine to 22 molecular operational taxonomic units (motus). The best scoring partition, asap score of 2.00 and P value of 1.00e-5, splits all samples into nine motus: local specimens into five and the Rocha-Olivares et al. (2001) into four. All 10 initial partitions of ABGD divide taxa into 10 motus, four recursive partitions split taxa into 14, 15, 25, and 32 motus. The highest scoring partitions suggest 10 motus: five for local specimens and five for the Rocha-Olivares et al. (2001) specimens (P value of 1.00e-01). mPTP splits the data into nine motus: five for local specimens and four included from the Rocha-Olivares et al. (2001) study. bPTP splits the data into 11 motus: local specimens into six and Rocha-Olivares et al. (2001) study into five. GMYC splits the data into eight or 11 motus, depending on the model and rate of

molecular evolution used to make the BEAST tree. The Yule model with constant and relaxed rates of molecular evolution group local taxa into six putative species and Rocha-Olivares et al. (2001) into five groups. The relaxed clock model splits local taxa and one of the Rocha-Olivares et al. (2001) sequences into five groups, and four of the Rocha-Olivares et al. (2001) samples into three groups, this is the only model that groups one of the Rocha-Olivares et al. (2001) sequences with local taxa.

Cletocamptus

Species delimitation analysis yields three lineages of *Cletocamptus* in the CRLs, and at least five lineages of *Cletocamptus* in all sampled coastal lagoons. As in other studies, different methods of genetic species delimitation produce different results (Hofmann et al. 2019; Guimarães et al. 2022; Ranasinghe et al. 2022). This is due to model assumption violations and/or to the varying statistical power of each model (Carstens et al. 2013).

Coastal saline lagoons in Puerto Rico harbor several genetic lineages of *Cletocamptus*; some of these are likely undescribed species. The presence of multiple putative species is congruent with recent studies of *Cletocamptus* (Gómez and Yáñez-Rivera 2022) and Harpacticoida in general (Karanovic and Cooper 2012;

TABLE 4. Mean genetic distances between lineages of *Cletocamptus* found in Puerto Rico, including the Rocha-Olivares et al. (2001) sequences (*C. stimpsoni, C. fourchensis, C. deborahdexterae, C. sinaloensis,* and *C. helobius*). Numbers 1–5 denote groups yielded by ML phylogenetic analysis of COI gene. The lower matrix triangle shows the corrected distances, and the upper one shows the uncorrected *p*-distance.

	PR-1	PR-2	PR-3	PR-4	PR-5	*C. sinaloensis*	*C. deborah-dexterae*	*C. fourchensis*	*C. stimpsoni*	*C. helobius*	*Stenocaris* sp.
PR-1		0.26	0.26	0.25	0.26	0.27	0.26	0.27	0.27	0.23	0.27
PR-2	0.42		0.21	0.2	0.19	0.22	0.21	0.19	0.21	0.21	0.22
PR-3	0.43	0.3		0.22	0.2	0.22	0.22	0.22	0.24	0.25	0.25
PR-4	0.38	0.28	0.33		0.11	0.19	0.18	0.21	0.24	0.26	0.25
PR-5	0.42	0.27	0.29	0.13		0.21	0.19	0.23	0.24	0.27	0.25
C. sinaloensis	0.43	0.32	0.33	0.26	0.3		0.09	0.22	0.26	0.27	0.26
C. deborahdexterae	0.43	0.31	0.34	0.25	0.27	0.10		0.22	0.25	0.27	0.27
C. fourchensis	0.46	0.27	0.32	0.31	0.34	0.33	0.33		0.23	0.24	0.24
C. stimpsoni	0.44	0.3	0.38	0.38	0.39	0.43	0.39	0.35		0.25	0.26
C. helobius	0.35	0.3	0.39	0.42	0.42	0.43	0.44	0.36	0.38		0.23
Stenocaris sp.	0.44	0.32	0.4	0.39	0.38	0.42	0.46	0.37	0.43	0.34	

TABLE 5. Presence of each *Cletocamptus* lineage at each location in Puerto Rico as defined by the ML multigene phylogeny.

Lineage	Cabo Rojo	Providencia	Encarnación	Punta Petrona	Flamenco
1	✓	✓			✓
2	✓		✓		
3				✓	
4	✓	✓	✓	✓	✓
5		✓	✓		✓

Rossel and Martínez Arbizu 2019; Vakati et al. 2019) where careful examination of material yields a higher level of standing diversity than previously thought.

CONCLUSION

Harpacticoid copepods play a key role in aquatic trophic dynamics, both as primary and secondary consumers, and as a significant food source for many larger invertebrates and vertebrates (Williamson and Reid 2009; Baguley et al. 2019). *Cletocamptus* copepods are highly abundant in the Cabo Rojo lagoons of Puerto Rico, reaching up to 1,300 copepods/cm². Given the high abundances these copepods reach, they should be considered essential components of the trophic dynamics and carbon fluxes of these coastal lagoons, an important stopover for migratory shorebirds in the Caribbean (Miller and Lugo 2009). No significant correlation
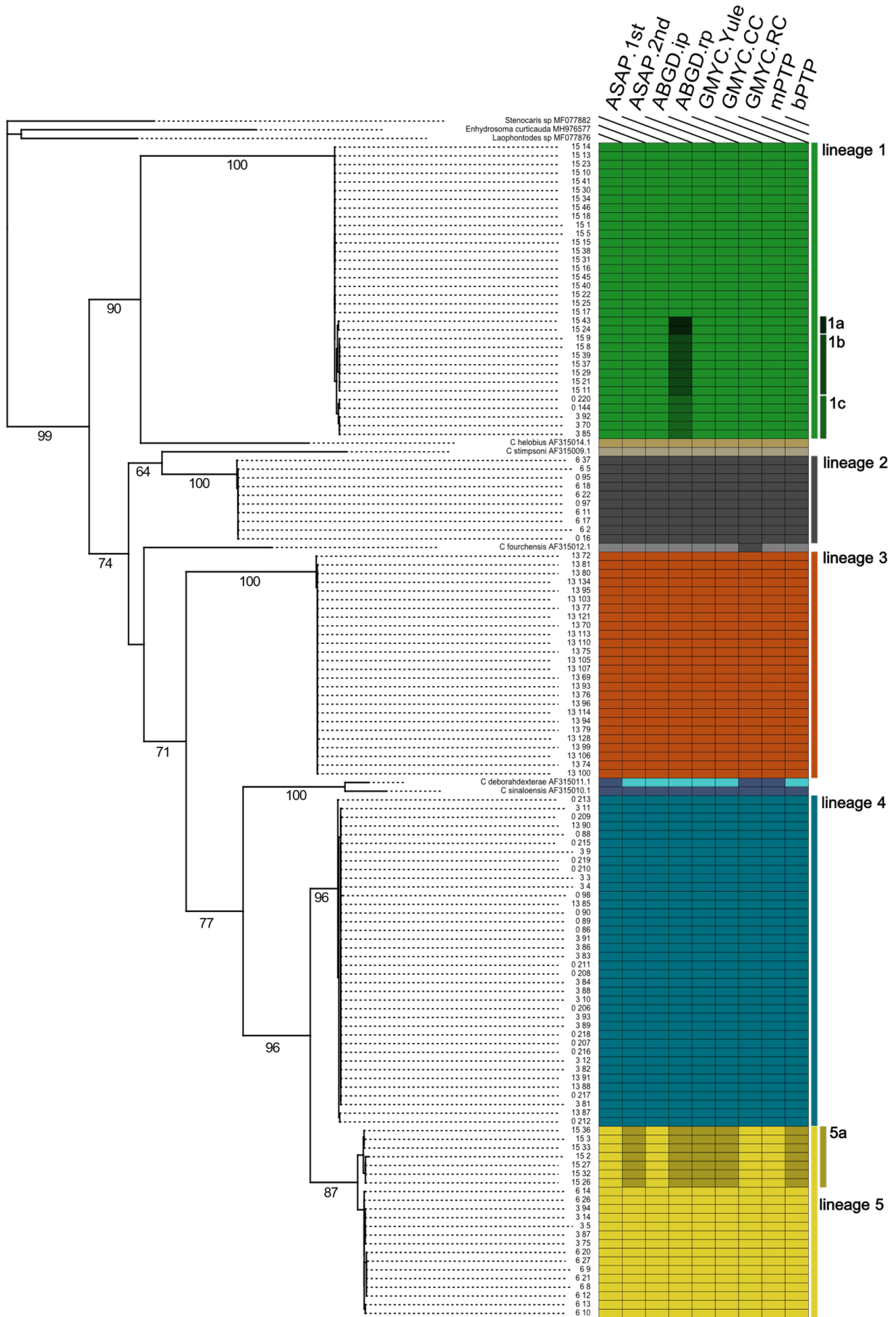
[Previous page] FIG. 9. Maximum likelihood phylogenetic tree constructed using COI sequences, annotated with species delimitation results. Colors represent putative lineages identified by the 1st and 2nd best ASAP results; initial and recursive partitions of ABGD; Yule, Constant Coalescent, and Relaxed Clock models for GMYC; mPTP; and bPTP. Numbers below branches indicate bootstrap values, while numbers at node tips correspond to individual copepod specimens. The tree was created with IQ-TREE (Minh et al. 2020)last accessed February 6, 2020, and annotations were made using the R v. 4.2.2 2 (RStudio Team 2020; R Core Team 2021) package of *Phytools* v. 1.5.3 (Revell 2012).

between their abundances and factors: lagoon, area, or sampling time was found, meaning that the variability of the abundances at each lagoon area was independent throughout sampling times. The physicochemical parameters considered in this study did not correlate with abundances either. As such, copepods were observed to be tolerant to wide fluctuations in salinity, i.e., 27 to 135 psu, and can thrive in euhaline and hypersaline conditions.

Large genetic distances between the lineages, clear phylogenetic groupings, and consistent groupings yielded by species delimitation software indicate that coastal saline lagoons in Puerto Rico hold at least four genetic lineages/species of *Cletocamptus*. Some of these lineages exhibit patterns of genetic differentiation attributed to spatial barriers, i.e., isolation of lagoons. Such diversity is an unexpected result, as we originally started this project to study *Cletocamptus dominicanus*, the only reported species at that time, with the initial hypothesis of no geographic differentiation due to the small sampling area and widespread distribution of these copepods. However, our finding of multiple putative species is congruent with recent studies of *Cletocamptus* and of Harpacticoida in general, where careful examination of material yields high levels of genetic divergence.

In summary, understanding the ecological context and distribution of organisms is crucial for understanding their evolution and diversity. The potential for spatial barriers to drive genetic differentiation and speciation in aquatic organisms highlights the importance of understanding the connectivity and distribution of populations for their conservation and management. This study contributes to the ecology of the genus *Cletocamptus* in Puerto Rico by showing that these remarkable harpacticoid copepods are halotolerant and thrive in extreme environments and highlights the potential of using the hypersaline conditions of the coastal lagoons of Puerto Rico as natural laboratories to study mechanisms of adaptation in these extreme environments in

terms of salinity and temperature, which co-varies with salinity. It also contributes to the study of biodiversity and systematics within the genus *Cletocamptus*, by creating genetic resources for species that may have no formal morphological description, yet. Given the importance, ephemeral nature, and vulnerability of these coastal lagoons, it is pressing to study and protect their biota and habitat.

LITERATURE CITED

Adamowicz, S. J., S. Menu-Marque, S. A. Halse, J. C. Topan, T. S. Zemlak, P. D. N. Hebert, and J. D. S. Witt. 2010. The evolutionary diversification of the Centropagidae (Crustacea, Calanoida): A history of habitat shifts. *Molecular Phylogenetics and Evolution* 55: 418–430.

Alcocer, J., M. de. C. Hernández, L. A. Oseguera, and E. Escobar. 2015. On the ecology of *Cletocamptus gomezi* Suárez-Morales, Barrera-Moreno & Ciros-Pérez 2013 (Crustacea, Copepoda, Harpacticoida) micro-endemic to Lake Alchichica, Central Mexico. *Journal of Limnology* 74: 302–309.

Altschul, S. F., W. Gish, W. Miller, E. W. Myers, and D. J. Lipman. 1990. Basic local alignment search tool. *Journal of Molecular Biology* 215: 403–410.

FIG. 10 [First half]. Maximum likelihood phylogeny based on 28S sequences, created using IQ-TREE (Minh et al. 2020)last accessed February 6, 2020. Tip labels represent sequences from *Cletocamptus* sequences generated in this study, numbers next to branches represent bootstrap values.
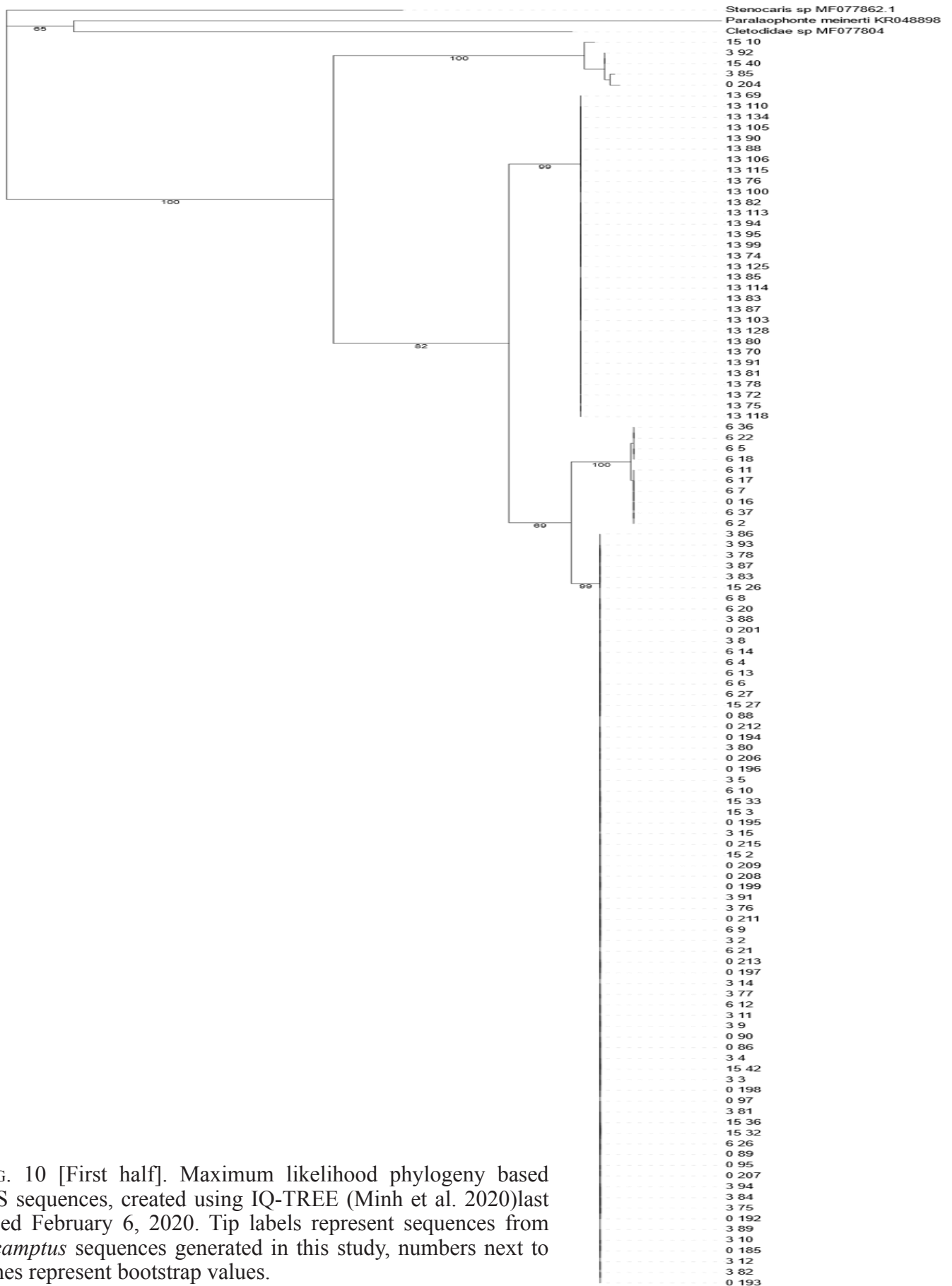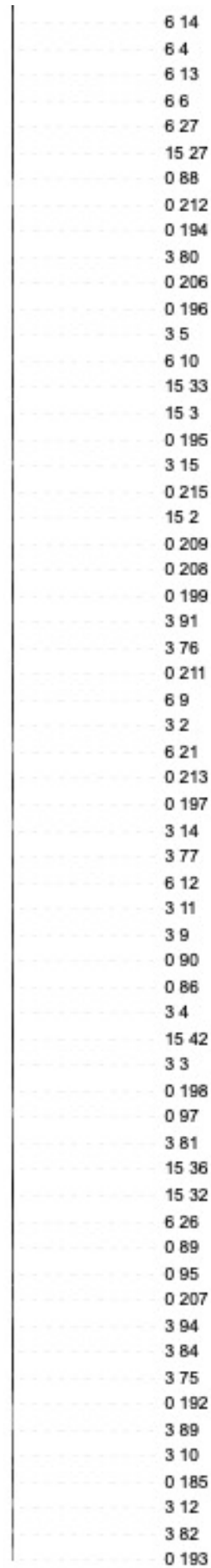
FIG. 10 [Second half]. Maximum likelihood phylogeny based on 28S sequences, created using IQ-TREE (Minh et al. 2020)last accessed February 6, 2020. Tip labels represent sequences from *Cletocamptus* sequences generated in this study, numbers next to branches represent bootstrap values.
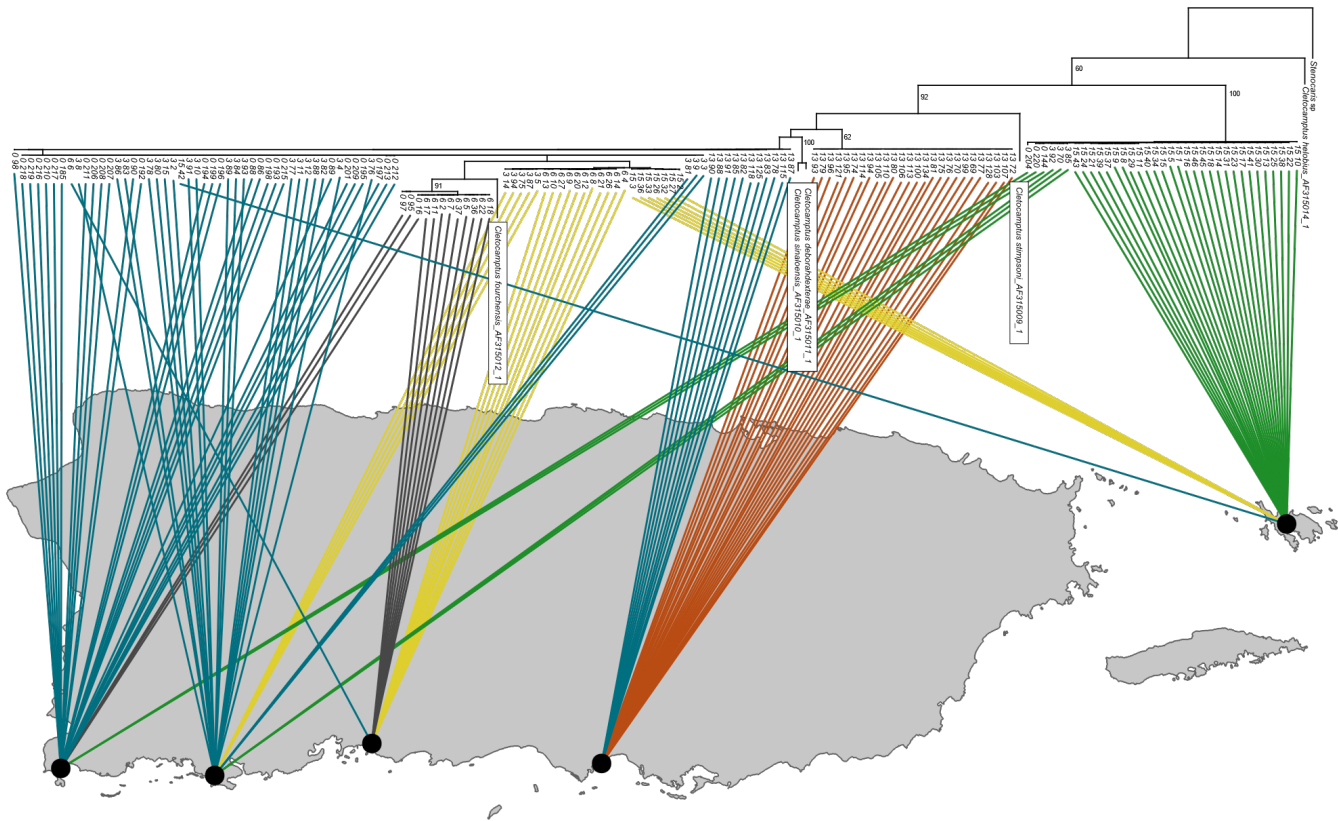
FIG. 11. Multigene ML phylogeny overlaid on a map of Puerto Rico. The phylogenetic tree was constructed using IQ-TREE (Minh et al. 2020) with concatenated COI and 28S sequences, including those from Rocha-Olivares et al. (2001). *Stenocaris* sp. was used as an outgroup. Each tip represents a single copepod specimen, with colored lines linking specimens to their sampling locations. Green, gray, red, blue, and yellow represent lineages 1 through 5, respectively; phylogenetic groups were rearranged for clarity on the map. Numbers next to branches represent bootstrap values. The figure was created using the R v. 4.2.2 2 (RStudio Team 2020; R Core Team 2021) package of Phytools v. 1.5.3 (Revell 2012).

Anderson, M. J., R. N. Gorley, and K. R. Clarke. 2008. PERMANOVA+ for PRIMER: Guide to Software and Statistical Methods. Pp. 1–214 in *Plymouth, UK*. Available from: http://www.primer-e.com

Anufriieva, E. V. 2014. Copepods in Hypersaline Waters Worldwide: Diversity, Environmental, Social, and Economic Roles. *Acta Geologica Sinica - English Edition* 88: 43–45.

Anufriieva, E. V. 2015. Do copepods inhabit hypersaline waters worldwide? A short review and discussion. *Chinese Journal of Oceanology and Limnology* 33: 1354–1361.

Armenteros, M., J. P. Williams, B. Creagh, and N. Capetillo. 2007. Spatial and temporal variations of meiofaunal communities from the western sector of the Gulf of Batabanó, Cuba: III. Vertical distribution. *Revista de Biología Tropical* 56: 1127–1134.

Baguley, J. G., B. C. Coull, and G. T. Chandler. 2019. Meiobenthos. Pp. 742–748 in *Encyclopedia of Ocean Sciences*, *3*(June).

Bucklin, A., B. D. Ortman, R. M. Jennings, L. M. Nigro, C. J. Sweetman, N. J. Copley, T. Sutton, and P. H. Wiebe. 2010. A "Rosetta Stone" for metazoan zooplankton: DNA barcode analysis of species diversity of the Sargasso Sea (Northwest Atlantic Ocean). *Deep-Sea Research Part II: Topical Studies in Oceanography* 57: 2234–2247.

Capella-Gutiérrez, S., J. M. Silla-Martínez, and T. Gabaldón. 2009. trimAl: A tool for automated alignment trimming in large-scale phylogenetic analyses. *Bioinformatics* 25: 1972–1973.

Carstens, B. C., T. A. Pelletier, N. M. Reid, and J. D. Satler. 2013. How to fail at species delimitation. *Molecular Ecology* 22: 4369–4383.

Castro-Longoria, E., J. L. Alvarez-Borrego, A. Rocha-Olivares, S. Gómez, and V. Kober. 2003. Power of a multidisciplinary approach: Use of morphological, molecular and digital methods in the study of

harpacticoid cryptic species. *Marine Ecology Progress Series* 249: 297–303.

Clarke, K. R. and R. N. Gorley. 2015. *PRIMER v7: User Manual/Tutorial* [Computer software]. PRIMER-E Ltd Registered.

Collazo, J. A., B. A. Harrington, J. S. Grear, and J. A. Colón. 1995. Abundance and Distribution of Shorebirds at the Cabo Rojo Salt Flats, Puerto Rico (Abundancia y Distribución de Playeros en las Salinas de Cabo Rojo, Puerto Rico). *Journal of Field Ornithology* 66: 424–438.

Dahms, H. U. and P. Y. Qian. 2004. Life histories of the Harpacticoida (Copepoda, Crustacea): A comparison with meiofauna and macrofauna. *Journal of Natural History* 38: 1725–1734.

De Troch, M., L. Houthoofd, V. Chepurnov, and A. Vanreusel. 2006. Does sediment grain size affect diatom grazing by harpacticoid copepods? *Marine Environmental Research* 61: 265–277.

Ezard, T., T. Fujisawa, and T. Barraclough. 2021. *splits: SPecies' LImits by Threshold Statistics* [Computer software]. Available at: https://r-forge.r-project.org/projects/splits/

Fleeger, J. W. 1980. Morphological Variation in *Cletocamptus* (Copepoda: Harpacticoida), with Description of a New Species from Louisiana Salt Marshes. *Transactions of the American Microscopical Society* 99: 25–31.

Folmer, O., M. Black, W. Hoeh, R. Lutz, and R. Vrijenhoek. 1994. DNA primers for amplification of mitochondrial cytochrome c oxidase subunit I from diverse metazoan invertebrates. *Molecular Marine Biology and Biotechnology* 3: 294–299.

Frangoulis, C., E. D. Christou, and J. H. Hecq. 2004. Comparison of marine copepod outfluxes: Nature, rate, fate and role in the carbon and nitrogen cycles. *Advances in Marine Biology* 47: 253–309.

Frisch, D., A. J. Green, and J. Figuerola. 2007. High dispersal capacity of a broad spectrum of aquatic invertebrates via waterbirds. *Aquatic Sciences* 69: 568–574.

Fujisawa, T. and T. G. Barraclough. 2013. Delimiting species using single-locus data and the generalized mixed yule coalescent approach: A revised method and evaluation on simulated data sets. *Systematic Biology* 62: 707–724.

Garlitska, L., T. Neretina, D. Schepetov, N. Mugue, M.

De Troch, J. G. Baguley, and A. Azovsky. 2012. Cryptic diversity of the "cosmopolitan" harpacticoid copepod *Nannopus palustris*: Genetic and morphological evidence. *Molecular Ecology* 21: 5336–5347.

Geller, J., C. Meyer, M. Parker, and H. Hawk. 2013. Redesign of PCR primers for mitochondrial cytochrome c oxidase subunit I for marine invertebrates and application in all-taxa biotic surveys. *Molecular Ecology Resources* 13: 851–861.

Gómez, S., J. W. Fleeger, A. Rocha-Olivares, and D. Foltz. 2004. Four new species of *Cletocamptus* Schmankevitsch, 1875, closely related to *Cletocamptus deitersi* (Richard, 1897) (Copepoda: Harpacticoida). *Journal of Natural History* 38: 2669–2732.

Gómez, S., R. Gerber, and J. M. Fuentes-Reinés. 2017. Redescription of *Cletocamptus albuquerquensis* and *C. dominicanus* (Harpacticoida: Canthocamptidae incertae sedis), and description of two new species from the US Virgin Islands and Bonaire. *Zootaxa* 4272: 301–359.

Gómez, S., B. Ingole, M. Sawant, and R. Singh. 2013. *Cletocamptus goenchim* sp. Nov., a new harpacticoid (Copepoda: Harpacticoida) from India. *Proceedings of the Biological Society of Washington* 126: 259–275.

Gómez, S., R. Scheihing, and P. Labarca. 2007. A new species of *Cletocamptus* (Copepoda: Harpacticoida) from Chile and some notes on *Cletocamptus axi* Mielke, 2000. *Journal of Natural History* 41: 39–60.

Gómez, S. and B. Yáñez-Rivera. 2022. The genus *Cletocamptus* (Harpacticoida, Canthocamptidae): A reappraisal, with proposal of a new subfamily, a new genus, and a new species. *ZooKeys* 2022: 165–208.

González, C. E., E. Goetze, R. Escribano, O. Ulloa, and P. Victoriano. 2020. Genetic diversity and novel lineages in the cosmopolitan copepod *Pleuromamma abdominalis* in the Southeast Pacific. *Scientific Reports* 10: 1–15.

Green, A. J. and J. Figuerola. 2005. Recent advances in the study of long-distance dispersal of aquatic invertebrates via birds. *Diversity and Distributions* 11: 149–156.

Guimarães, K. L. A., M. P. Lima, D. J. Santana, M. F. B. de Souza, R. S. Barbosa, and L. R. R. Rodrigues.

2022. DNA barcoding and phylogeography of the *Hoplias malabaricus* species complex. *Scientific Reports* 12: 1–15.

Hebert, P. D. N., A. Cywinska, S. L. Ball, and J. R. DeWaard. 2003. Biological identifications through DNA barcodes. *Proceedings of the Royal Society B: Biological Sciences* 270: 313–321.

Hellberg, M. E. 2009. Gene Flow and Isolation among Populations of Marine Animals. *Annual Review of Ecology, Evolution, and Systematics* 40: 291–310.

Hessen, D. O., T. C. Jensen, and B. Walseng. 2019. Zooplankton diversity and dispersal by birds; Insights from different geographical scales. *Frontiers in Ecology and Evolution* 7: 1–11.

Hicks, G. R. F. and B. C. Coull. 1983. The ecology of marine meiobenthic harpacticoid copepods. *Oceanography and Marine Biology* 21: 67–175.

Hofmann, E. P., K. E. Nicholson, I. R. Luque-Montes, G. Köhler, C. A. Cerrato-Mendoza, M. Medina-Flores, L. D. Wilson, and J. H. Townsend. 2019. Cryptic diversity, but to what extent? Discordance between single-locus species delimitation methods within mainland anoles (Squamata: Dactyloidae) of northern Central America. *Frontiers in Genetics* 10: 1–13.

Huelsenbeck, J. P. and F. Ronquist. 2001. MRBAYES: Bayesian inference of phylogenetic trees. *Bioinformatics* 17: 754–755.

Jayabarathi, R., G. Padmavati, and I. Anandavelu. 2015. Spatial heterogeneity of benthic copepods: A comparative aspect on composition, abundance, and correlation. *Zoological Studies* 54: 51.

Jensen, P. 1982. A new meiofauna sample splitter. *Annales Zoologici Fennici* 19: 233–236.

Kalyaanamoorthy, S., B. Q. Minh, T. K. F. Wong, A. Von Haeseler, and L. S. Jermiin. 2017. ModelFinder: Fast model selection for accurate phylogenetic estimates. *Nature Methods* 14: 587–589.

Kapli, P., S. Lutteropp, J. Zhang, K. Kobert, P. Pavlidis, A. Stamatakis, and T. Flouri. 2017. Multi-rate Poisson tree processes for single-locus species delimitation under maximum likelihood and Markov chain Monte Carlo. *Bioinformatics* 33: 1630–1638.

Karanovic, T. and S. J. B. Cooper. 2012. Explosive radiation of the genus *Schizopera* on a small subterranean island in Western Australia (Copepoda:Harpacticoida): Unravelling the cases of cryptic speciation, size differentiation and multiple invasions. *Invertebrate Systematics* 26: 115–192.

Katoh, K., J. Rozewicki, and K. D. Yamada. 2019. MAFFT online service: Multiple sequence alignment, interactive sequence choice and visualization. *Briefings in Bioinformatics* 20: 1160–1166.

Kikuchi, Y. 1994. *Glaciella*, a new genus of freshwater Canthocamptidae (Copepoda, Harpacticoida) from a glacier in Nepal, Himalayas. *Hydrobiologia* 292–293: 59–66.

Larsson, A. 2014. AliView: A fast and lightweight alignment viewer and editor for large datasets. *Bioinformatics* 30: 3276–3278.

Lee, E. H., S. Y. Choi, M. H. Seo, S. J. Lee, and H. Y. Soh. 2020. Effects of Temperature and pH on the Egg Production and Hatching Success of a Common Korean Copepod. *Diversity* 12: 372.

Leray, M., J. Y. Yang, C. P. Meyer, S. C. Mills, N. Agudelo, V. Ranwez, J. T. Boehm, and R. J. Machida. 2013. A new versatile primer set targeting a short fragment of the mitochondrial COI region for metabarcoding metazoan diversity: Application for characterizing coral reef fish gut contents. *Frontiers in Zoology* 10: 1–14.

Letunic, I. and P. Bork. 2021. Interactive tree of life (iTOL) v5: An online tool for phylogenetic tree display and annotation. *Nucleic Acids Research* 49: W293–W296.

Ma, Z., J. Ren, and R. Zhang. 2022. Identifying the Genetic Distance Threshold for Entiminae (Coleoptera: Curculionidae) Species Delimitation via COI Barcodes. *Insects* 13: 261.

Machida, R. J., M. U. Miya, M. Nishida, and S. Nishida. 2006. Molecular phylogeny and evolution of the pelagic copepod genus *Neocalanus* (Crustacea: Copepoda). *Marine Biology* 148: 1071–1079.

Meyer, C. P. 2003. Molecular systematics of cowries (Gastropoda: Cypraeidae) and diversification patterns in the tropics. *Biological Journal of the Linnean Society* 79: 401–459.

Michels, J. and M. Büntzow. 2010. Assessment of Congo red as a fluorescence marker for the exoskeleton of small crustaceans and the cuticle of polychaetes. *Journal of Microscopy* 238: 95–101.

Michonneau, F. 2016. *Using GMYC for species delination*. Zenodo. Available at: https://doi.org/10.5281/zenodo.838260

Miller, G. L. and A. E. Lugo. 2009. Guide to the ecological systems of Puerto Rico. *General Technical Report IITF-GTR-35*: 1–436.

Minh, B. Q., H. A. Schmidt, O. Chernomor, D. Schrempf, M. D. Woodhams, A. Von Haeseler, R. Lanfear, and E. Teeling. 2020. IQ-TREE 2: New Models and Efficient Methods for Phylogenetic Inference in the Genomic Era. *Molecular Biology and Evolution* 37: 1530–1534.

Ortman, B. D. 2008. DNA Barcoding the Medusozoa and Ctenophora. University of Connecticut, Dissertation. Available at: https://www.proquest.com/dissertations-theses/dna-barcoding-medusozoa-ctenophora/docview/304626674/se-2

Parks, M. A., J. A. Collazo, J. A. Colón, K. R. Ramos Álvarez, and O. Díaz. 2016. Change in Numbers of Resident and Migratory Shorebirds at the Cabo Rojo Salt Flats, Puerto Rico, USA (1985–2014). *Waterbirds* 39: 209–214.

Puillandre, N., S. Brouillet, and G. Achaz. 2021. ASAP: assemble species by automatic partitioning. *Molecular Ecology Resources* 21: 609–620.

Puillandre, N., A. Lambert, S. Brouillet, and G. Achaz. 2012. ABGD, Automatic Barcode Gap Discovery for primary species delimitation. *Molecular Ecology* 21: 1864–1877.

R Core Team. 2021. *R: A Language and Environment for Statistical Computing*. R Foundation for Statistical Computing. Available at: https://www.r-project.org/

Ranasinghe, U. G. S. L., J. Eberle, J. Thormann, C. Bohacz, S. P. Benjamin, and D. Ahrens. 2022. Multiple species delimitation approaches with COI barcodes poorly fit each other and morphospecies – An integrative taxonomy case of Sri Lankan *Sericini chafers* (Coleoptera: Scarabaeidae). *Ecology and Evolution* 12: 1–15.

Revell, L. J. 2012. phytools: An R package for phylogenetic comparative biology (and other things). *Methods in Ecology and Evolution* 3: 217–223).

Rocha-Olivares, A., J. W. Fleeger, and D. W. Foltz. 2001. Decoupling of molecular and morphological evolution in deep lineages of a meiobenthic harpacticoid copepod. *Molecular Biology and Evolution* 18: 1088–1102.

Rosli, N., D. Leduc, A. A. Rowden, and P. K. Probert. 2018. Review of recent trends in ecological studies of deep-sea meiofauna, with focus on patterns and processes at small to regional spatial scales. *Marine Biodiversity* 48: 13–34.

Rossel, S. and P. Martínez Arbizu. 2019. Revealing higher than expected diversity of Harpacticoida (Crustacea:Copepoda) in the North Sea using MALDI-TOF MS and molecular barcoding. *Scientific Reports* 9: 1–14.

RStudio Team. 2020. *RStudio: Integrated Development Environment for R* [Computer software]. RStudio. Available at: http://www.rstudio.com/

Schratzberger, M. adn J. Ingels. 2018. Meiofauna matters: The roles of meiofauna in benthic ecosystems. *Journal of Experimental Marine Biology and Ecology* 502: 12–25.

Seifried, S. 2004. The importance of a phylogenetic system for the study of deep-sea harpacticoid diversity. *Zoological Studies* 43: 435–445.

Shadrin, N. V. and E. V. Anufriieva. 2013. Dependence of *Arctodiaptomus salinus* (Calanoida, Copepoda) halotolerance on exoosmolytes: New data and a hypothesis. *Journal of Mediterranean Ecology* 12: 21–26.

Suárez-Morales, E. 2015. Class Maxillopoda. Pp. 709–755 in *Thorp and Covich's Freshwater Invertebrates* (Vol. 1). Elsevier.

Súarez-Morales, E., O. Barrera-Moreno, and J. Ciros-Pérez. 2013. A new species of *Cletocamptus* Schmankewitsch, 1875 (Crustacea, Copepoda, Harpacticoida) from a high altitude saline lake in Central Mexico. *Journal of Limnology* 72: 313–325.

Tamura, K., G. Stecher, and S. Kumar. 2021. MEGA11: Molecular Evolutionary Genetics Analysis Version 11. *Molecular Biology and Evolution* 38: 3022–3027.

Turner, J. T. 2004. The importance of small pelagic planktonic copepods and their roles in pelagic marine food webs. *Zoological Studies* 43: 255–266.

Vakati, V., S. Eyun, and W. Lee. 2019. Unraveling the intricate biodiversity of the benthic harpacticoid genus *Nannopus* (Copepoda, Harpacticoida, Nannopodidae) in Korean waters. *Molecular Phylogenetics and Evolution* 130: 366–379.

Von Weissenberg, E., G. Mottola, T.-M. Uurasmaa, K. Anttila, and J. Engström-Öst. 2022. Combined effect of salinity and temperature on copepod reproduction and oxidative stress in brackish-water en-

vironment. *Frontiers in Marine Science* 9: 952863.

Williamson, C. E. and J. W. Reid. 2009. Copepoda. Pp. 633–642 in *Encyclopedia of Inland Waters*. Elsevier.

WoRMS Editorial Board. 2024. World Register of Marine Species. Available from: https://www.marine-species.org.

Yakovenko, V., N. Shadrin, and E. Anufriieva. 2024. Interannual differences vs small-scale spatiotemporal variability of spring zooplankton in the Crime-an marine hypersaline lake. *Continental Shelf Research* 282: 105338.

Yamamuro, M. 2000. Abundance and size distribution of sublittoral meiobenthos along estuarine salinity gradients. *Journal of Marine Systems* 26: 135–143.

Zhang, J., P. Kapli, P. Pavlidis, and A. Stamatakis. 2013. A general species delimitation method with applications to phylogenetic placements. *Bioinformatics* 29: 2869–2876.

Appendix 1a. COI GenBank accession numbers and associated collection data; all specimens are from Puerto Rico; JPD = J. P. Domenech, AG = A. González, LV = Liz Vega, NS = N. Schizas.

Voucher #	Coordinates	Sex	Collected by	Date	Locality	Accession	GI
0_144	17.956305, -67.211543	female	JPD, AG	08-DEC-2019	Cabo Rojo: Laguna Candelaria	OQ682378.1	2463908584
0_16	17.944309, -67.192303	female	JPD, AG	08-DEC-2019	Cabo Rojo: Laguna Sucia	OQ682339.1	2463908468
0_206	17.947031, -67.192559	female	JPD	14-SEP-2018	Cabo Rojo: Laguna Fraternidad	OQ682315.1	2463908405
0_207	17.947031, -67.192559	female	JPD	14-SEP-2018	Cabo Rojo: Laguna Fraternidad	OQ682316.1	2463908408
0_208	17.947031, -67.192559	female	JPD	14-SEP-2018	Cabo Rojo: Laguna Fraternidad	OQ682317.1	2463908410
0_209	17.947031, -67.192559	female	JPD	14-SEP-2018	Cabo Rojo: Laguna Fraternidad	OQ682336.1	2463908460
0_210	17.947031, -67.192559	female	JPD	14-SEP-2018	Cabo Rojo: Laguna Fraternidad	OQ682318.1	2463908413
0_211	17.947031, -67.192559	female	JPD	14-SEP-2018	Cabo Rojo: Laguna Fraternidad	OQ682319.1	2463908415
0_212	17.947031, -67.192559	female	JPD	14-SEP-2018	Cabo Rojo: Laguna Fraternidad	OQ682301.1	2463908370
0_213	17.947031, -67.192559	female	JPD	14-SEP-2018	Cabo Rojo: Laguna Fraternidad	OQ682303.1	2463908375
0_215	17.947031, -67.192559	female	JPD	14-SEP-2018	Cabo Rojo: Laguna Fraternidad	OQ682337.1	2463908463
0_216	17.947031, -67.192559	female	JPD	14-SEP-2018	Cabo Rojo: Laguna Fraternidad	OQ682320.1	2463908417
0_217	17.947031, -67.192559	female	JPD	14-SEP-2018	Cabo Rojo: Laguna Fraternidad	OQ682321.1	2463908420
0_218	17.947031, -67.192559	female	JPD	14-SEP-2018	Cabo Rojo: Laguna Fraternidad	OQ682322.1	2463908422
0_219	17.947031, -67.192559	female	JPD	14-SEP-2018	Cabo Rojo: Laguna Fraternidad	OQ682323.1	2463908425
0_220	17.947031, -67.192559	female	JPD	14-SEP-2018	Cabo Rojo: Laguna Fraternidad	OQ682379.1	2463908587
0_86	17.947031, -67.192559	female	JPD	14-SEP-2018	Cabo Rojo: Laguna Fraternidad	OQ682307.1	2463908385
0_88	17.947031, -67.192559	female	JPD	14-SEP-2018	Cabo Rojo: Laguna Fraternidad	OQ682305.1	2463908380
0_89	17.947031, -67.192559	female	JPD	14-SEP-2018	Cabo Rojo: Laguna Fraternidad	OQ682308.1	2463908388
0_90	17.947031, -67.192559	female	JPD	14-SEP-2018	Cabo Rojo: Laguna Fraternidad	OQ682309.1	2463908390
0_95	17.947031, -67.192559	female	JPD	14-SEP-2018	Cabo Rojo: Laguna Fraternidad	OQ682347.1	2463908497
0_97	17.947031, -67.192559	female	JPD	14-SEP-2018	Cabo Rojo: Laguna Fraternidad	OQ682344.1	2463908481
0_98	17.947031, -67.192559	female	JPD	14-SEP-2018	Cabo Rojo: Laguna Fraternidad	OQ682338.1	2463908466
13_100	17.96006, -66.36575	female	JPD, LV	02-APR-2021	Santa Isabel: Laguna Punta Petrona	OQ682349.1	2463908503
13_103	17.96006, -66.36575	female	JPD, LV	02-APR-2021	Santa Isabel: Laguna Punta Petrona	OQ682350.1	2463908506
13_105	17.96006, -66.36575	female	JPD, LV	02-APR-2021	Santa Isabel: Laguna Punta Petrona	OQ682351.1	2463908508
13_106	17.96006, -66.36575	female	JPD, LV	02-APR-2021	Santa Isabel: Laguna Punta Petrona	OQ682352.1	2463908511
13_107	17.96006, -66.36575	female	JPD, LV	02-APR-2021	Santa Isabel: Laguna Punta Petrona	OQ682353.1	2463908513
13_110	17.96006, -66.36575	female	JPD, LV	02-APR-2021	Santa Isabel: Laguna Punta Petrona	OQ682354.1	2463908516
13_113	17.96006, -66.36575	female	JPD, LV	02-APR-2021	Santa Isabel: Laguna Punta Petrona	OQ682355.1	2463908519
13_114	17.96006, -66.36575	female	JPD, LV	02-APR-2021	Santa Isabel: Laguna Punta Petrona	OQ682369.1	2463908560
13_121	17.96006, -66.36575	female	JPD, LV	02-APR-2021	Santa Isabel: Laguna Punta Petrona	OQ682356.1	2463908521
13_128	17.96006, -66.36575	female	JPD, LV	02-APR-2021	Santa Isabel: Laguna Punta Petrona	OQ682373.1	2463908570
13_134	17.96006, -66.36575	female	JPD, LV	02-APR-2021	Santa Isabel: Laguna Punta Petrona	OQ682357.1	2463908525

13_69	17.96006, -66.36575	female	JPD, LV	02-APR-2021	Santa Isabel: Laguna Punta Petrona	OQ682358.1	2463908529
13_70	17.96006, -66.36575	female	JPD, LV	02-APR-2021	Santa Isabel: Laguna Punta Petrona	OQ682359.1	2463908532
13_72	17.96006, -66.36575	female	JPD, LV	02-APR-2021	Santa Isabel: Laguna Punta Petrona	OQ682374.1	2463908573
13_74	17.96006, -66.36575	female	JPD, LV	02-APR-2021	Santa Isabel: Laguna Punta Petrona	OQ682370.1	2463908562
13_75	17.96006, -66.36575	female	JPD, LV	02-APR-2021	Santa Isabel: Laguna Punta Petrona	OQ682360.1	2463908535
13_76	17.96006, -66.36575	female	JPD, LV	02-APR-2021	Santa Isabel: Laguna Punta Petrona	OQ682361.1	2463908538
13_77	17.96006, -66.36575	female	JPD, LV	02-APR-2021	Santa Isabel: Laguna Punta Petrona	OQ682371.1	2463908565
13_79	17.96006, -66.36575	female	JPD, LV	02-APR-2021	Santa Isabel: Laguna Punta Petrona	OQ682362.1	2463908541
13_80	17.96006, -66.36575	female	JPD, LV	02-APR-2021	Santa Isabel: Laguna Punta Petrona	OQ682363.1	2463908544
13_81	17.96006, -66.36575	female	JPD, LV	02-APR-2021	Santa Isabel: Laguna Punta Petrona	OQ682364.1	2463908547
13_85	17.96006, -66.36575	female	JPD, LV	02-APR-2021	Santa Isabel: Laguna Punta Petrona	OQ682310.1	2463908392
13_87	17.96006, -66.36575	female	JPD, LV	02-APR-2021	Santa Isabel: Laguna Punta Petrona	OQ682302.1	2463908373
13_88	17.96006, -66.36575	female	JPD, LV	02-APR-2021	Santa Isabel: Laguna Punta Petrona	OQ682311.1	2463908395
13_90	17.96006, -66.36575	female	JPD, LV	02-APR-2021	Santa Isabel: Laguna Punta Petrona	OQ682312.1	2463908398
13_91	17.96006, -66.36575	female	JPD, LV	02-APR-2021	Santa Isabel: Laguna Punta Petrona	OQ682313.1	2463908400
13_93	17.96006, -66.36575	female	JPD, LV	02-APR-2021	Santa Isabel: Laguna Punta Petrona	OQ682372.1	2463908567
13_94	17.96006, -66.36575	female	JPD, LV	02-APR-2021	Santa Isabel: Laguna Punta Petrona	OQ682365.1	2463908550
13_95	17.96006, -66.36575	female	JPD, LV	02-APR-2021	Santa Isabel: Laguna Punta Petrona	OQ682366.1	2463908553
13_96	17.96006, -66.36575	female	JPD, LV	02-APR-2021	Santa Isabel: Laguna Punta Petrona	OQ682367.1	2463908556
13_99	17.96006, -66.36575	female	JPD, LV	02-APR-2021	Santa Isabel: Laguna Punta Petrona	OQ682368.1	2463908558
15_1	18.32665, -65.31479	female	JPD, NS	17-AUG-2022	Culebra: Laguna Flamenco	OQ682392.1	2463908625
15_10	18.32665, -65.31479	female	JPD, NS	17-AUG-2022	Culebra: Laguna Flamenco	OQ682380.1	2463908590
15_11	18.32665, -65.31479	female	JPD, NS	17-AUG-2022	Culebra: Laguna Flamenco	OQ682400.1	2463908647
15_13	18.32665, -65.31479	female	JPD, NS	17-AUG-2022	Culebra: Laguna Flamenco	OQ682381.1	2463908593
15_14	18.32665, -65.31479	female	JPD, NS	17-AUG-2022	Culebra: Laguna Flamenco	OQ682391.1	2463908622
15_15	18.32665, -65.31479	female	JPD, NS	17-AUG-2022	Culebra: Laguna Flamenco	OQ682399.1	2463908643
15_16	18.32665, -65.31479	female	JPD, NS	17-AUG-2022	Culebra: Laguna Flamenco	OQ682382.1	2463908597
15_17	18.32665, -65.31479	female	JPD, NS	17-AUG-2022	Culebra: Laguna Flamenco	OQ682383.1	2463908599
15_18	18.32665, -65.31479	female	JPD, NS	17-AUG-2022	Culebra: Laguna Flamenco	OQ682384.1	2463908602
15_2	18.32665, -65.31479	female	JPD, NS	17-AUG-2022	Culebra: Laguna Flamenco	OQ682300.1	2463908368
15_21	18.32665, -65.31479	female	JPD, NS	17-AUG-2022	Culebra: Laguna Flamenco	OQ682401.1	2463908650
15_22	18.32665, -65.31479	female	JPD, NS	17-AUG-2022	Culebra: Laguna Flamenco	OQ682393.1	2463908627
15_23	18.32665, -65.31479	female	JPD, NS	17-AUG-2022	Culebra: Laguna Flamenco	OQ682396.1	2463908635
15_24	18.32665, -65.31479	female	JPD, NS	17-AUG-2022	Culebra: Laguna Flamenco	OQ682407.1	2463908667
15_25	18.32665, -65.31479	female	JPD, NS	17-AUG-2022	Culebra: Laguna Flamenco	OQ682385.1	2463908606
15_26	18.32665, -65.31479	female	JPD, NS	17-AUG-2022	Culebra: Laguna Flamenco	OQ682294.1	2463908352
15_27	18.32665, -65.31479	female	JPD, NS	17-AUG-2022	Culebra: Laguna Flamenco	OQ682296.1	2463908357
15_29	18.32665, -65.31479	female	JPD, NS	17-AUG-2022	Culebra: Laguna Flamenco	OQ682402.1	2463908652
15_3	18.32665, -65.31479	female	JPD, NS	17-AUG-2022	Culebra: Laguna Flamenco	OQ682299.1	2463908365
15_30	18.32665, -65.31479	female	JPD, NS	17-AUG-2022	Culebra: Laguna Flamenco	OQ682397.1	2463908638
15_31	18.32665, -65.31479	female	JPD, NS	17-AUG-2022	Culebra: Laguna Flamenco	OQ682386.1	2463908608
15_32	18.32665, -65.31479	female	JPD, NS	17-AUG-2022	Culebra: Laguna Flamenco	OQ682295.1	2463908355
15_33	18.32665, -65.31479	female	JPD, NS	17-AUG-2022	Culebra: Laguna Flamenco	OQ682297.1	2463908360
15_34	18.32665, -65.31479	female	JPD, NS	17-AUG-2022	Culebra: Laguna Flamenco	OQ682398.1	2463908640
15_36	18.32665, -65.31479	female	JPD, NS	17-AUG-2022	Culebra: Laguna Flamenco	OQ682298.1	2463908362
15_37	18.32665, -65.31479	female	JPD, NS	17-AUG-2022	Culebra: Laguna Flamenco	OQ682403.1	2463908656
15_38	18.32665, -65.31479	female	JPD, NS	17-AUG-2022	Culebra: Laguna Flamenco	OQ682394.1	2463908630
15_39	18.32665, -65.31479	female	JPD, NS	17-AUG-2022	Culebra: Laguna Flamenco	OQ682404.1	2463908659

15_40	18.32665, -65.31479	female	JPD, NS	17-AUG-2022	Culebra: Laguna Flamenco	OQ682387.1	2463908610
15_41	18.32665, -65.31479	female	JPD, NS	17-AUG-2022	Culebra: Laguna Flamenco	OQ682388.1	2463908613
15_43	18.32665, -65.31479	female	JPD, NS	17-AUG-2022	Culebra: Laguna Flamenco	OQ682408.1	2463908669
15_45	18.32665, -65.31479	female	JPD, NS	17-AUG-2022	Culebra: Laguna Flamenco	OQ682389.1	2463908615
15_46	18.32665, -65.31479	female	JPD, NS	17-AUG-2022	Culebra: Laguna Flamenco	OQ682390.1	2463908619
15_5	18.32665, -65.31479	female	JPD, NS	17-AUG-2022	Culebra: Laguna Flamenco	OQ682395.1	2463908632
15_8	18.32665, -65.31479	female	JPD, NS	17-AUG-2022	Culebra: Laguna Flamenco	OQ682406.1	2463908664
15_9	18.32665, -65.31479	female	JPD, NS	17-AUG-2022	Culebra: Laguna Flamenco	OQ682405.1	2463908661
3_10	17.9417, -66.95926	female	JPD, LV	02-APR-2021	Guánica: Laguna Providencia	OQ682324.1	2463908428
3_11	17.9417, -66.95926	female	JPD, LV	02-APR-2021	Guánica: Laguna Providencia	OQ682335.1	2463908457
3_12	17.9417, -66.95926	female	JPD, LV	02-APR-2021	Guánica: Laguna Providencia	OQ682332.1	2463908449
3_14	17.9417, -66.95926	female	JPD, LV	02-APR-2021	Guánica: Laguna Providencia	OQ682284.1	2463908327
3_3	17.9417, -66.95926	female	JPD, LV	02-APR-2021	Guánica: Laguna Providencia	OQ682325.1	2463908430
3_4	17.9417, -66.95926	female	JPD, LV	02-APR-2021	Guánica: Laguna Providencia	OQ682326.1	2463908432
3_5	17.9417, -66.95926	female	JPD, LV	02-APR-2021	Guánica: Laguna Providencia	OQ682286.1	2463908332
3_70	17.9417, -66.95926	female	JPD, LV	02-APR-2021	Guánica: Laguna Providencia	OQ682377.1	2463908580
3_75	17.9417, -66.95926	female	JPD, LV	02-APR-2021	Guánica: Laguna Providencia	OQ682282.1	2463908321
3_81	17.9417, -66.95926	female	JPD, LV	02-APR-2021	Guánica: Laguna Providencia	OQ682304.1	2463908377
3_82	17.9417, -66.95926	female	JPD, LV	02-APR-2021	Guánica: Laguna Providencia	OQ682314.1	2463908403
3_83	17.9417, -66.95926	female	JPD, LV	02-APR-2021	Guánica: Laguna Providencia	OQ682306.1	2463908383
3_84	17.9417, -66.95926	female	JPD, LV	02-APR-2021	Guánica: Laguna Providencia	OQ682327.1	2463908435
3_85	17.9417, -66.95926	female	JPD, LV	02-APR-2021	Guánica: Laguna Providencia	OQ682375.1	2463908575
3_86	17.9417, -66.95926	female	JPD, LV	02-APR-2021	Guánica: Laguna Providencia	OQ682328.1	2463908438
3_87	17.9417, -66.95926	female	JPD, LV	02-APR-2021	Guánica: Laguna Providencia	OQ682283.1	2463908324
3_88	17.9417, -66.95926	female	JPD, LV	02-APR-2021	Guánica: Laguna Providencia	OQ682329.1	2463908441
3_89	17.9417, -66.95926	female	JPD, LV	02-APR-2021	Guánica: Laguna Providencia	OQ682334.1	2463908454
3_9	17.9417, -66.95926	female	JPD, LV	02-APR-2021	Guánica: Laguna Providencia	OQ682333.1	2463908452
3_91	17.9417, -66.95926	female	JPD, LV	02-APR-2021	Guánica: Laguna Providencia	OQ682330.1	2463908443
3_92	17.9417, -66.95926	female	JPD, LV	02-APR-2021	Guánica: Laguna Providencia	OQ682376.1	2463908578
3_93	17.9417, -66.95926	female	JPD, LV	02-APR-2021	Guánica: Laguna Providencia	OQ682331.1	2463908447
3_94	17.9417, -66.95926	female	JPD, LV	02-APR-2021	Guánica: Laguna Providencia	OQ682285.1	2463908329
6_10	17.99063, -66.7182	female	JPD, LV	02-APR-2021	Peñuelas: Laguna Encarnación	OQ682279.1	2463908314
6_11	17.99063, -66.7182	female	JPD, LV	02-APR-2021	Peñuelas: Laguna Encarnación	OQ682343.1	2463908478
6_12	17.99063, -66.7182	female	JPD, LV	02-APR-2021	Peñuelas: Laguna Encarnación	OQ682288.1	2463908337
6_13	17.99063, -66.7182	female	JPD, LV	02-APR-2021	Peñuelas: Laguna Encarnación	OQ682280.1	2463908316
6_14	17.99063, -66.7182	female	JPD, LV	02-APR-2021	Peñuelas: Laguna Encarnación	OQ682287.1	2463908334
6_17	17.99063, -66.7182	female	JPD, LV	02-APR-2021	Peñuelas: Laguna Encarnación	OQ682342.1	2463908476
6_18	17.99063, -66.7182	female	JPD, LV	02-APR-2021	Peñuelas: Laguna Encarnación	OQ682345.1	2463908483
6_2	17.99063, -66.7182	female	JPD, LV	02-APR-2021	Peñuelas: Laguna Encarnación	OQ682340.1	2463908471
6_20	17.99063, -66.7182	female	JPD, LV	02-APR-2021	Peñuelas: Laguna Encarnación	OQ682289.1	2463908339
6_21	17.99063, -66.7182	female	JPD, LV	02-APR-2021	Peñuelas: Laguna Encarnación	OQ682290.1	2463908342
6_22	17.99063, -66.7182	female	JPD, LV	02-APR-2021	Peñuelas: Laguna Encarnación	OQ682346.1	2463908494
6_26	17.99063, -66.7182	female	JPD, LV	02-APR-2021	Peñuelas: Laguna Encarnación	OQ682281.1	2463908319
6_27	17.99063, -66.7182	female	JPD, LV	02-APR-2021	Peñuelas: Laguna Encarnación	OQ682293.1	2463908350
6_37	17.99063, -66.7182	female	JPD, LV	02-APR-2021	Peñuelas: Laguna Encarnación	OQ682348.1	2463908500
6_5	17.99063, -66.7182	female	JPD, LV	02-APR-2021	Peñuelas: Laguna Encarnación	OQ682341.1	2463908473
6_8	17.99063, -66.7182	female	JPD, LV	02-APR-2021	Peñuelas: Laguna Encarnación	OQ682291.1	2463908345
6_9	17.99063, -66.7182	female	JPD, LV	02-APR-2021	Peñuelas: Laguna Encarnación	OQ682292.1	2463908347

APPENDIX 1b. 28S GenBank accession numbers and associated collection data; all specimens are from Puerto Rico; JPD = J. P. Domenech, AG = A. González, LV = Liz Vega, NS = N. Schizas.

Voucher #	Coordinates	Sex	Collected by	Date	Locality	Accession	GI
0_16	17.944309, -67.192303	female	JPD, AG	08-DEC-2019	Cabo Rojo: Laguna Fraternidad	OQ819183.1	2486667153
0_185	17.947031, -67.192559	female	JPD	14-SEP-2018	Cabo Rojo: Laguna Fraternidad	OQ819193.1	2486667163
0_192	17.947031, -67.192559	male	JPD	14-SEP-2018	Cabo Rojo: Laguna Fraternidad	OQ819194.1	2486667164
0_193	17.947031, -67.192559	female	JPD	14-SEP-2018	Cabo Rojo: Laguna Fraternidad	OQ819195.1	2486667165
0_194	17.947031, -67.192559	female	JPD	14-SEP-2018	Cabo Rojo: Laguna Fraternidad	OQ819196.1	2486667166
0_195	17.947031, -67.192559	male	JPD	14-SEP-2018	Cabo Rojo: Laguna Fraternidad	OQ819197.1	2486667167
0_196	17.947031, -67.192559	female	JPD	14-SEP-2018	Cabo Rojo: Laguna Fraternidad	OQ819198.1	2486667168
0_197	17.947031, -67.192559	male	JPD	14-SEP-2018	Cabo Rojo: Laguna Fraternidad	OQ819199.1	2486667169
0_198	17.947031, -67.192559	male	JPD	14-SEP-2018	Cabo Rojo: Laguna Fraternidad	OQ819200.1	2486667170
0_199	17.947031, -67.192559	female	JPD	14-SEP-2018	Cabo Rojo: Laguna Fraternidad	OQ819201.1	2486667171
0_201	17.947031, -67.192559	female	JPD	14-SEP-2018	Cabo Rojo: Laguna Fraternidad	OQ819202.1	2486667172
0_204	17.947031, -67.192559	female	JPD	14-SEP-2018	Cabo Rojo: Laguna Fraternidad	OQ819295.1	2486667265
0_206	17.947031, -67.192559	female	JPD	14-SEP-2018	Cabo Rojo: Laguna Fraternidad	OQ819203.1	2486667173
0_207	17.947031, -67.192559	female	JPD	14-SEP-2018	Cabo Rojo: Laguna Fraternidad	OQ819204.1	2486667174
0_208	17.947031, -67.192559	female	JPD	14-SEP-2018	Cabo Rojo: Laguna Fraternidad	OQ819205.1	2486667175
0_209	17.947031, -67.192559	female	JPD	14-SEP-2018	Cabo Rojo: Laguna Fraternidad	OQ819206.1	2486667176
0_211	17.947031, -67.192559	female	JPD	14-SEP-2018	Cabo Rojo: Laguna Fraternidad	OQ819207.1	2486667177
0_212	17.947031, -67.192559	female	JPD	14-SEP-2018	Cabo Rojo: Laguna Fraternidad	OQ819208.1	2486667178
0_213	17.947031, -67.192559	female	JPD	14-SEP-2018	Cabo Rojo: Laguna Fraternidad	OQ819209.1	2486667179
0_215	17.947031, -67.192559	female	JPD	14-SEP-2018	Cabo Rojo: Laguna Fraternidad	OQ819210.1	2486667180
0_86	17.947031, -67.192559		JPD	14-SEP-2018	Cabo Rojo: Laguna Fraternidad	OQ819211.1	2486667181
0_88	17.947031, -67.192559	female	JPD	14-SEP-2018	Cabo Rojo: Laguna Fraternidad	OQ819212.1	2486667182
0_89	17.947031, -67.192559		JPD	14-SEP-2018	Cabo Rojo: Laguna Fraternidad	OQ819213.1	2486667183
0_90	17.947031, -67.192559		JPD	14-SEP-2018	Cabo Rojo: Laguna Fraternidad	OQ819214.1	2486667184
0_95	17.947031, -67.192559	female	JPD	14-SEP-2018	Cabo Rojo: Laguna Fraternidad	OQ819215.1	2486667185
0_97	17.947031, -67.192559	female	JPD	14-SEP-2018	Cabo Rojo: Laguna Fraternidad	OQ819216.1	2486667186
13_100	17.96006, -66.36575	female	JPD, LV	02-APR-2021	Santa Isabel: Laguna Punta Petrona	OQ819264.1	2486667234
13_103	17.96006, -66.36575	female	JPD, LV	02-APR-2021	Santa Isabel: Laguna Punta Petrona	OQ819265.1	2486667235
13_105	17.96006, -66.36575	female	JPD, LV	02-APR-2021	Santa Isabel: Laguna Punta Petrona	OQ819266.1	2486667236
13_106	17.96006, -66.36575	female	JPD, LV	02-APR-2021	Santa Isabel: Laguna Punta Petrona	OQ819267.1	2486667237
13_110	17.96006, -66.36575	female	JPD, LV	02-APR-2021	Santa Isabel: Laguna Punta Petrona	OQ819268.1	2486667238
13_113	17.96006, -66.36575	female	JPD, LV	02-APR-2021	Santa Isabel: Laguna Punta Petrona	OQ819269.1	2486667239
13_114	17.96006, -66.36575	female	JPD, LV	02-APR-2021	Santa Isabel: Laguna Punta Petrona	OQ819270.1	2486667240
13_115	17.96006, -66.36575	female	JPD, LV	02-APR-2021	Santa Isabel: Laguna Punta Petrona	OQ819271.1	2486667241
13_118	17.96006, -66.36575		JPD, LV	02-APR-2021	Santa Isabel: Laguna Punta Petrona	OQ819272.1	2486667242
13_125	17.96006, -66.36575	male	JPD, LV	02-APR-2021	Santa Isabel: Laguna Punta Petrona	OQ819273.1	2486667243
13_128	17.96006, -66.36575	female	JPD, LV	02-APR-2021	Santa Isabel: Laguna Punta Petrona	OQ819274.1	2486667244
13_134	17.96006, -66.36575	female	JPD, LV	02-APR-2021	Santa Isabel: Laguna Punta Petrona	OQ819275.1	2486667245
13_69	17.96006, -66.36575	female	JPD, LV	02-APR-2021	Santa Isabel: Laguna Punta Petrona	OQ819276.1	2486667246
13_70	17.96006, -66.36575	female	JPD, LV	02-APR-2021	Santa Isabel: Laguna Punta Petrona	OQ819277.1	2486667247
13_72	17.96006, -66.36575	female	JPD, LV	02-APR-2021	Santa Isabel: Laguna Punta Petrona	OQ819278.1	2486667248
13_74	17.96006, -66.36575	female	JPD, LV	02-APR-2021	Santa Isabel: Laguna Punta Petrona	OQ819279.1	2486667249
13_75	17.96006, -66.36575	female	JPD, LV	02-APR-2021	Santa Isabel: Laguna Punta Petrona	OQ819280.1	2486667250
13_76	17.96006, -66.36575	female	JPD, LV	02-APR-2021	Santa Isabel: Laguna Punta Petrona	OQ819281.1	2486667251

13_78	17.96006, -66.36575		JPD, LV	02-APR-2021	Santa Isabel: Laguna Punta Petrona	OQ819282.1	2486667252
13_80	17.96006, -66.36575	female	JPD, LV	02-APR-2021	Santa Isabel: Laguna Punta Petrona	OQ819283.1	2486667253
13_81	17.96006, -66.36575	female	JPD, LV	02-APR-2021	Santa Isabel: Laguna Punta Petrona	OQ819284.1	2486667254
13_82	17.96006, -66.36575		JPD, LV	02-APR-2021	Santa Isabel: Laguna Punta Petrona	OQ819285.1	2486667255
13_83	17.96006, -66.36575	female	JPD, LV	02-APR-2021	Santa Isabel: Laguna Punta Petrona	OQ819286.1	2486667256
13_85	17.96006, -66.36575	female	JPD, LV	02-APR-2021	Santa Isabel: Laguna Punta Petrona	OQ819287.1	2486667257
13_87	17.96006, -66.36575	female	JPD, LV	02-APR-2021	Santa Isabel: Laguna Punta Petrona	OQ819288.1	2486667258
13_88	17.96006, -66.36575	female	JPD, LV	02-APR-2021	Santa Isabel: Laguna Punta Petrona	OQ819289.1	2486667259
13_90	17.96006, -66.36575	female	JPD, LV	02-APR-2021	Santa Isabel: Laguna Punta Petrona	OQ819290.1	2486667260
13_91	17.96006, -66.36575	female	JPD, LV	02-APR-2021	Santa Isabel: Laguna Punta Petrona	OQ819291.1	2486667261
13_94	17.96006, -66.36575	female	JPD, LV	02-APR-2021	Santa Isabel: Laguna Punta Petrona	OQ819292.1	2486667262
13_95	17.96006, -66.36575	female	JPD, LV	02-APR-2021	Santa Isabel: Laguna Punta Petrona	OQ819293.1	2486667263
13_99	17.96006, -66.36575	female	JPD, LV	02-APR-2021	Santa Isabel: Laguna Punta Petrona	OQ819294.1	2486667264
15_10	18.32665, -65.31479	female	JPD, NS	17-AUG-2022	Culebra: Laguna Flamenco	OQ819299.1	2486667269
15_2	18.32665, -65.31479	female	JPD, NS	17-AUG-2022	Culebra: Laguna Flamenco	OQ819219.1	2486667189
15_26	18.32665, -65.31479	female	JPD, NS	17-AUG-2022	Culebra: Laguna Flamenco	OQ819217.1	2486667187
15_27	18.32665, -65.31479		JPD, NS	17-AUG-2022	Culebra: Laguna Flamenco	OQ819218.1	2486667188
15_3	18.32665, -65.31479	female	JPD, NS	17-AUG-2022	Culebra: Laguna Flamenco	OQ819223.1	2486667193
15_32	18.32665, -65.31479	female	JPD, NS	17-AUG-2022	Culebra: Laguna Flamenco	OQ819220.1	2486667190
15_33	18.32665, -65.31479	female	JPD, NS	17-AUG-2022	Culebra: Laguna Flamenco	OQ819221.1	2486667191
15_36	18.32665, -65.31479	female	JPD, NS	17-AUG-2022	Culebra: Laguna Flamenco	OQ819222.1	2486667192
15_40	18.32665, -65.31479	female	JPD, NS	17-AUG-2022	Culebra: Laguna Flamenco	OQ819296.1	2486667266
15_42	18.32665, -65.31479	male	JPD, NS	17-AUG-2022	Culebra: Laguna Flamenco	OQ819224.1	2486667194
3_10	17.9417, -66.95926	female	JPD, LV	02-APR-2021	Guánica: Laguna Providencia	OQ819225.1	2486667195
3_11	17.9417, -66.95926	female	JPD, LV	02-APR-2021	Guánica: Laguna Providencia	OQ819262.1	2486667232
3_12	17.9417, -66.95926	female	JPD, LV	02-APR-2021	Guánica: Laguna Providencia	OQ819226.1	2486667196
3_14	17.9417, -66.95926	female	JPD, LV	02-APR-2021	Guánica: Laguna Providencia	OQ819227.1	2486667197
3_15	17.9417, -66.95926		JPD, LV	02-APR-2021	Guánica: Laguna Providencia	OQ819263.1	2486667233
3_2	17.9417, -66.95926	female	JPD, LV	02-APR-2021	Guánica: Laguna Providencia	OQ819228.1	2486667198
3_3	17.9417, -66.95926	female	JPD, LV	02-APR-2021	Guánica: Laguna Providencia	OQ819229.1	2486667199
3_4	17.9417, -66.95926	female	JPD, LV	02-APR-2021	Guánica: Laguna Providencia	OQ819230.1	2486667200
3_5	17.9417, -66.95926	female	JPD, LV	02-APR-2021	Guánica: Laguna Providencia	OQ819231.1	2486667201
3_75	17.9417, -66.95926	female	JPD, LV	02-APR-2021	Guánica: Laguna Providencia	OQ819232.1	2486667202
3_76	17.9417, -66.95926		JPD, LV	02-APR-2021	Guánica: Laguna Providencia	OQ819233.1	2486667203
3_77	17.9417, -66.95926	female	JPD, LV	02-APR-2021	Guánica: Laguna Providencia	OQ819234.1	2486667204
3_78	17.9417, -66.95926	female	JPD, LV	02-APR-2021	Guánica: Laguna Providencia	OQ819235.1	2486667205
3_8	17.9417, -66.95926	female	JPD, LV	02-APR-2021	Guánica: Laguna Providencia	OQ819245.1	2486667215
3_80	17.9417, -66.95926	female	JPD, LV	02-APR-2021	Guánica: Laguna Providencia	OQ819236.1	2486667206
3_81	17.9417, -66.95926	female	JPD, LV	02-APR-2021	Guánica: Laguna Providencia	OQ819237.1	2486667207
3_82	17.9417, -66.95926	female	JPD, LV	02-APR-2021	Guánica: Laguna Providencia	OQ819238.1	2486667208
3_83	17.9417, -66.95926	female	JPD, LV	02-APR-2021	Guánica: Laguna Providencia	OQ819239.1	2486667209
3_84	17.9417, -66.95926	female	JPD, LV	02-APR-2021	Guánica: Laguna Providencia	OQ819240.1	2486667210
3_85	17.9417, -66.95926	female	JPD, LV	02-APR-2021	Guánica: Laguna Providencia	OQ819298.1	2486667268
3_86	17.9417, -66.95926	female	JPD, LV	02-APR-2021	Guánica: Laguna Providencia	OQ819241.1	2486667211
3_87	17.9417, -66.95926	female	JPD, LV	02-APR-2021	Guánica: Laguna Providencia	OQ819242.1	2486667212
3_88	17.9417, -66.95926	female	JPD, LV	02-APR-2021	Guánica: Laguna Providencia	OQ819243.1	2486667213
3_89	17.9417, -66.95926	female	JPD, LV	02-APR-2021	Guánica: Laguna Providencia	OQ819244.1	2486667214

3_9	17.9417, -66.95926	female	JPD, LV	02-APR-2021	Guánica: Laguna Providencia	OQ819249.1	2486667219
3_91	17.9417, -66.95926	female	JPD, LV	02-APR-2021	Guánica: Laguna Providencia	OQ819246.1	2486667216
3_92	17.9417, -66.95926	female	JPD, LV	02-APR-2021	Guánica: Laguna Providencia	OQ819297.1	2486667267
3_93	17.9417, -66.95926	female	JPD, LV	02-APR-2021	Guánica: Laguna Providencia	OQ819247.1	2486667217
3_94	17.9417, -66.95926	female	JPD, LV	02-APR-2021	Guánica: Laguna Providencia	OQ819248.1	2486667218
6_10	17.99063, -66.7182	female	JPD, LV	02-APR-2021	Peñuelas: Laguna Encarnación	OQ819250.1	2486667220
6_11	17.99063, -66.7182	female	JPD, LV	02-APR-2021	Peñuelas: Laguna Encarnación	OQ819184.1	2486667154
6_12	17.99063, -66.7182	female	JPD, LV	02-APR-2021	Peñuelas: Laguna Encarnación	OQ819251.1	2486667221
6_13	17.99063, -66.7182	female	JPD, LV	02-APR-2021	Peñuelas: Laguna Encarnación	OQ819252.1	2486667222
6_14	17.99063, -66.7182	female	JPD, LV	02-APR-2021	Peñuelas: Laguna Encarnación	OQ819253.1	2486667223
6_17	17.99063, -66.7182		JPD, LV	02-APR-2021	Peñuelas: Laguna Encarnación	OQ819185.1	2486667155
6_18	17.99063, -66.7182	female	JPD, LV	02-APR-2021	Peñuelas: Laguna Encarnación	OQ819189.1	2486667159
6_2	17.99063, -66.7182		JPD, LV	02-APR-2021	Peñuelas: Laguna Encarnación	OQ819186.1	2486667156
6_20	17.99063, -66.7182	female	JPD, LV	02-APR-2021	Peñuelas: Laguna Encarnación	OQ819254.1	2486667224
6_21	17.99063, -66.7182	female	JPD, LV	02-APR-2021	Peñuelas: Laguna Encarnación	OQ819255.1	2486667225
6_22	17.99063, -66.7182	female	JPD, LV	02-APR-2021	Peñuelas: Laguna Encarnación	OQ819190.1	2486667160
6_26	17.99063, -66.7182	female	JPD, LV	02-APR-2021	Peñuelas: Laguna Encarnación	OQ819256.1	2486667226
6_27	17.99063, -66.7182	female	JPD, LV	02-APR-2021	Peñuelas: Laguna Encarnación	OQ819257.1	2486667227
6_36	17.99063, -66.7182	female	JPD, LV	02-APR-2021	Peñuelas: Laguna Encarnación	OQ819191.1	2486667161
6_37	17.99063, -66.7182		JPD, LV	02-APR-2021	Peñuelas: Laguna Encarnación	OQ819187.1	2486667157
6_4	17.99063, -66.7182		JPD, LV	02-APR-2021	Peñuelas: Laguna Encarnación	OQ819258.1	2486667228
6_5	17.99063, -66.7182	male	JPD, LV	02-APR-2021	Peñuelas: Laguna Encarnación	OQ819192.1	2486667162
6_6	17.99063, -66.7182		JPD, LV	02-APR-2021	Peñuelas: Laguna Encarnación	OQ819259.1	2486667229
6_7	17.99063, -66.7182	female	JPD, LV	02-APR-2021	Peñuelas: Laguna Encarnación	OQ819188.1	2486667158
6_8	17.99063, -66.7182	female	JPD, LV	02-APR-2021	Peñuelas: Laguna Encarnación	OQ819260.1	2486667230
6_9	17.99063, -66.7182		JPD, LV	02-APR-2021	Peñuelas: Laguna Encarnación	OQ819261.1	2486667231

APPENDIX 2. Average salinity (psu), pH, and temperature for each lagoon at each sampling time. The number in parentheses is the standard deviation.

Date	Lagoon	Salinity (psu)	pH	Temperature (° C)
2020-01-23	Candelaria	58 (12)	8.79 (0.22)	32 (0)
	Fraternidad	76 (3)	8.51 (0.05)	32 (1)
	Playa Sucia	60 (0)	8.96 (0.01)	33 (2)
2020-02-21	Candelaria	82 (43)	8.34 (0.12)	32 (3)
	Fraternidad	100 (11)	8.26 (0.02)	25 (2)
	Playa Sucia	79 (1)	8.51 (0.11)	27 (2)
2020-03-16	Candelaria	86 (6)	8.36 (0.11)	33 (1)
	Fraternidad	105 (13)	8.28 (0.07)	28 (5)
	Playa Sucia	87 (2)	8.51 (0.11)	33 (1)
2020-07-27	Candelaria	97 (19)	8.46 (0.18)	40 (2)
	Fraternidad	101 (55)	7.74 (0.38)	36 (3)
	Playa Sucia	90 (5)	8.29 (0.05)	38 (0)
2020-08-19	Candelaria	40 (8)	8.51 (0.15)	34 (2)
	Fraternidad	55 (11)	8.31 (0.12)	32 (1)
	Playa Sucia	55 (8)	8.09 (0.18)	31 (1)

2020-09-09	Candelaria	60 (17)	8.34 (0.15)	35 (2)
	Fraternidad	72 (17)	8.15 (0.15)	31 (1)
	Playa Sucia	58 (3)	8.26 (0.11)	31 (2)
2020-10-21	Candelaria	52 (16)	8.06 (0.04)	34 (3)
	Fraternidad	64 (2)	8.5 (0.08)	33 (3)
	Playa Sucia	59 (2)	8.51 (0.04)	37 (4)
2020-11-11	Candelaria	31 (4)	8.36 (0.17)	28 (1)
	Fraternidad	44 (6)	8.44 (0.02)	26 (1)
	Playa Sucia	41 (6)	8.58 (0.35)	26 (1)
2020-12-23	Candelaria	42 (7)	8.57 (0.63)	31 (3)
	Fraternidad	49 (12)	8.77 (0.16)	32 (2)
	Playa Sucia	46 (1)	8.54 (0.03)	33 (1)
2021-01-26	Candelaria	53 (18)	8.25 (0.31)	27 (3)
	Fraternidad	51 (14)	8.37 (0.29)	29 (1)
	Playa Sucia	53 (2)	8.28 (0.03)	31 (1)
2021-02-26	Candelaria	79 (41)	8.35 (0.23)	32 (3)
	Fraternidad	81 (38)	7.81 (0.53)	32 (3)
	Playa Sucia	81 (3)	8.33 (0.02)	32 (3)